STUDY ON PREVALENCE OF FELINE CORONAVIRUS AND FELINE INFECTIOUS PERITONITIS VIRUS IN THAILAND USING NESTED RT-PCR

INTRODUCTION

Feline infectious peritonitis virus (FIPV), a mutant of feline coronavirus (FCoV), infects domestic and wild feline of all species (Horzinek *et* al., 1979; Poland *et* al., 1996). FIPV causes a fatal systemic disease of feline called feline infectious peritonitis (FIP). The disease is characterized by Arthus-type immune response. FIP can be divided on the basis of fluid accumulation into two major forms, the effusive and non effusive forms (Pedersen *et* al., 1988). The most common clinical signs are non-specific and include fluctuating fever, inappetance, lethargy and weight loss.

FCoV is a member of the family *Coronaviridae.* The genome composes of five major open reading frames (ORFs), encoding polymerase, peplomer (S), envelope (E), matrix (M) and nucleocapsid (N) genes, respectively (Hohdatsu *et al*., 1998 b; Rottier, 1999). S gene is divides into S1 and S2 region (Vennema, 1999). The S1 region are more variable, containing various degrees of deletion and substitutions in different coronavirus strains or isolates (Pedersen, 1983).

FCoV can be distinguished on the basis of different virulence into two biotypes, avirulent strains (feline enteric coronavirus (FECV)) and virulent strain (FIPV) (Vennema, 1999; Janet *et al*., 1998; Pedersen, 1995 a). Both FECV and FIPV are very closely related so that they can not be distinguished by any serological methods (Janet *et al*., 1998; Barlough, 1985; Pedersen, 1976; Pedersen *et al*., 1981).

Recently, two nested reverse transcriptase PCR (RT-nPCR) were developed for the detection of FCoVs and FIPV (Herrewegh *et al*., 1995; Gamble *et al*., 1997). The FCoV RT-nPCR was developed for the detection of coronavirus RNA in serum, plasma,

ascitic fluids, tissues and feces of infected cats. The assay is targeted to the 3'-untranslated region (3'-UTR) of the viral genome, which are 97 to 100% homologous among FCoV isolates. FIPV RT-nPCR was developed for the detection of FIPV in clinical fluid samples. The target sequence for the assay is in the S1 region of S gene that has sufficient sequence homology among FIPV strains. This assay is able to differentiate FIPV from FECV presenting in body fluids but not in other clinical specimens (Gamble *et al.*, 1997).

Up to date, there is no report of the presence of FCoV and FIPV in Thailand. Thus, in this study, we used the previously developed RT-PCR to study prevalence of FCoV and FIPV in sera of cats from the central part of Thailand.

Objective

The objective of this study is to evaluate the prevalence of FCoV and FIPV in the central and eastern part of Thailand using RT-PCR.

LITERATURE REVIEWS

Classification of Coronaviruses

The order Nidovirales consists of two families, Coronaviridae and Arteriviridae. The member of this order is a group of enveloped, positive-sense single-stranded RNA viruses. The family Coronaviridae includes the genera Coronavirus and Torovirus that differ in genome length, structural proteins and nuleocapsid structure but share many features of genome organization and replication strategy (Rottier, 1999). Despite containing similar genome organization, Arteriviruses have icosahedral nucleocapsids and markedly smaller genome than coronaviruses (Flint *et al*., 2000).

Coronaviruses are large and enveloped. Their nuclear material is positive-sense single-stranded RNA or mRNA like. They cause a range of diseases in farm and domestic animals, highly prevalent respiratory and enteric diseases in humans, other mammals and birds (Lili *et al*., 2000). They have the largest genomes of all RNA viruses and replicate by a unique mechanism. Virions mature by budding at intracellular membranes and infection with some coronaviruses induces cell fusion. The viral envelopes are studded with long, petal-shaped spikes, giving coronaviruses the appearance of a crown (corona in Latin) and the nucleocapsid are long, flexible helices containing the 27 to 30 kb genomic RNA (Figure 1) (Lai and Holmes, 2001).

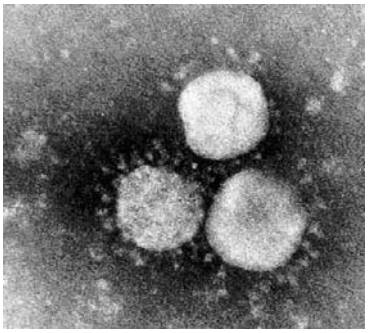

Figure 1 Electron micrograph showing human coronavirus 229E.

Source: Tyrrell and Myint (2006)

Physical properties of coronaviruses have been documented. Similar to other enveloped viruses, they are less stable in the environment and in clinical specimens than most nonenveloped viruses. When present in the environment, FCoV is easily labile. Infectivity is lost within 24-36 hours at room temperature, but can be maintained for many months as temperatures below -10 degrees Celsius (Pedersen, 1976). In general, coronavirus infectivity can be maintained at neutral or mildly acidic pH (Lai and Holmes, 2001). Disinfection of FCoV is readily inactivated by acid (pH3), heat (56 degrees Celsius for 1 hour), 0.2% formaldehyde and 3% bleach (Pedersen, 1976).

Coronaviruses can be grouped into three clusters on the basis of serology and genetic comparisons (Table 1). Within each group, the viruses are classified according to their natural host and diseases they produced (Lai and Holmes, 2001; Rottier, 1999). Most coronaviruses caused diseases only in one natural host species or a limited number of closely related species. Systemic infections of coronaviruses restricted to a few cell type, often the epithelial cell of the respiratory or enteric tracts and macrophages, causing localized infection (Table 1) (Lai and Holmes, 2001).

Table 1 Three groups of coronaviruses on the basis of serology

Antigenic group	Virus	Natural Host	Disease				
			Respiratory infection	Enteric infection	Hepatitis	Neurologic infection	Other[1]
I	CCoV	Dog		x			
	FECV	Cat		x			
	FIPV	Cat	x	x	x	x	x
	HCoV-229E	Human	x				
	PRCoV	Pig	x	x			x
	RbCoV	Rabbit		x			
	TGEV	Pig	x	x			x
II	BCoV	Cow	x	x			
	HCoV-OC43	Human	x				
	HEV	Pig	x	x		x	
	MHV	Mouse	x	x	x	x	
	SDAV	Rat					x
	TCoV	Turkey	x	x			
III	IBV	Chicken	x		x		x
	TCoV	Turkey	x	x			
Not grouped	SARS-CoV	Human	x				

[1]Other diseases caused by coronaviruses include infectious peritonitis, immunologic disorders, runting, nephritis, pancreatitis, parotitis, myocarditis and sialodacryoadenitis.

Note Explanation of acronyms, CCoV, canine coronavirus ; FECV, feline enteric coronavirus ; FIPV, feline infectious peritonitis virus ; HCoV-229E, human coronavirus 229E ; PRCoV, porcine respiratory coronavirus ; RbCoV, rabbit coronavirus ; TGEV, transmissible gastroenteritis virus ; BCoV, bovine coronavirus ; HCoV-OC43, human coronavirus OC43 ; HEV, hemagglutinating encephalomyelitis virus ; MHV, murine hepatitis virus ; SDAV, sialodacryoadenitis virus ; TCoV, turkey coronavirus ; IBV, infectious bronchitis virus ; SARS-CoV, severe acute respiratory syndrome coronavirus.

Source: Lai and Holmes (2001)

Feline Coronavirus

Feline coronaviruses (FCoV) is classified in the family Coronaviridae, order Nidovirales (Rottier, 1999). The morphology of FCoV is similar to other coronaviruses. The viral envelope is studded with long, petal-shaped spikes. Nuclear material is positive-sense single-stranded RNA viruses. The particles are pleomorphic, ranging from 75 to 250 nm or more in diameter (Pedersen, 1995). FCoV can be classified into serotype I and II according to their growth characteristics in cell culture and comparative degree of neutralization by antisera to canine coronavirus (CCoV) (Table 2) (Horzinek *et al*., 1995; Pedersen, 1995; Vennema *et al*., 1995). FCoVs of serotype II are genetically more closely related to CCoV than FCoVs of serotype I and they seem to have arisen by recombination between serotype I FCoV and CCoV (Motokawa et al., 1996; Vennema *et al*., 1995). FCoV serotype I is more prevalent serotype in field infections (Hohdatsu *et al*., 1992). FCoV are transmitted by the respiratory or enteric routes (Benbacer *et al*., 1997). Each serotype is capable of causing a spectrum of clinical sign in cats ranging from asymptomatic infections to diarrhea to feline infectious peritonitis (FIP).

Table 2 **Two serotype of FCoV on the basis growth characteristics in cell culture and comparative degree of neutralization by antisera to CCoV.**

Serotype	Growth characteristics in cell culture	Comparative degree of neutralization by antisera to CCoV
I	Difficult to grow, grows best in selective macrophage-like cell line, level of virus production in cell culture is low.	weakly
II	Easily to grow grows in many different cell line, produced in large amounts in cell culture.	strongly

Source: Horzinek *et al*. (1995)

Some FCoV isolates are unable to cause FIP when inoculated intraperitoneally into cats and were named feline enteric coronavirus (FECV) while feline infectious peritonitis virus (FIPV) can cause FIP. Therefore, in nature two biotypes of FCoV exist: FIPV and FECV, with different potential for causing disease. FECV strains can infect and replicate only in entrocytes of living cats, whereas FIPV can also grow in macrophages cell culture (Pedersen, 1995; Stoddart *et al*., 1989). Thus, different cell tropism of each virus may be a possible explanation of different manifestations of the disease. FECV causes diarrhea or asymptomatic infection, whereas FIPV leads to systemic infection, characterized by fibrinonecrotic and pyrogranulomatous peritonitis and pleuritis. FIPV can also spread to the central nervous system, where it causes granulomatous meningoencephalitis and uveitis (Tresnan, 1996).

Genetic comparison of FIPV and FECV isolates obtained from cats inhabiting the same environments shows high genetic similarity (Vennema *et al*., 1998). Sequence comparisons made from 1.2 to 8.9 kb segments on the 3'-end of the genome of FECV/FIPV pairs from the same catteries or shelter were 97.3-99.5% related. The mutations unique to FIPVs were found in open reading frames (ORFs) 3c and/or 7b and not mutations in the FECVs since similar sequences are present in other strains that have segregated earlier from a common ancestor. Therefore, FIPV may have arisen by mutation from endemic FECV (Vennema *et al*., 1998). Mutations are common in the 7b ORF of both type I and type II FECVs and may be associated with reduced virulence (Vennema *et al*., 1998). The 7b ORF encodes a nonstructural secretory glycoprotein of unknown function, which is not necessary for viral replication (Foley and Leutenegger, 2001). The actual rate of mutation may be affected by at least three different factors: (1) the level of FECV replication (the greater, the more chance for mutations to occur) (Poland *et al*., 1996), (2) the acquired or inherited resistance of the particular breed, bloodline, or individual cat to the mutant virus (Foley and Pedersen, 1995; Poland *et al*., 1996) and (3) the strain of FECV and the ease with which it can be mutated (Vennema *et al*., 1998).

Virion Morphology

The structure of coronavirus virions is spherical enveloped particles (Figure 2). Inside the virion is a single-stranded, positive-sense genomic RNA (Foley and Leutenegger, 2001; Rottier, 1999). The RNA genome is packaged by a nucleocapsid (N) phosphoprotein into helical ribonucleoprotein structures (Sturman *et al*., 1980). The nucleocapsid is incorporated into viral particles by budding through the membrane of the intermediate compartment between the endoplasmic reticulum and the Golgi complex (Kuo *et al*., 2000). Subsequent to budding, it may acquire a spherical and possibly icosahedral superstructure (Core). The virus core is enclosed by a lipoprotein envelope, which is formed during virus budding from intracellular membranes (Lai and Holmes, 2001). The virion envelope surrounding the nucleocapsid contained a minimal set of three structural proteins: the membrane glycoprotein (M), the small envelope protein (E) and the spike glycoprotein (S). In some coronaviruses, hemagglutinin-esterase glycoprotein (HE) may also be present, which is lacking in FCoV (Rottier, 1999). M is the most abundant protein of the virion structural protein. It spans the membrane bilayer three times, having a short amino-terminal domain on the exterior of virus and a large carboxy-terminus, containing more than half the mass of the molecule, in the virion interior (Kuo *et al*., 2000). Thus the M protein is apparently a component of both the internal core structure and the envelope (Lai and Holmes, 2001). The internal core composed of M (membrane) glycoprotein and probably N protein as well (Lai and Holmes, 2001). By contrast, E is a minor structural protein which is present in much smaller amounts than the other viral envelope proteins (Vennema *et al*., 1995). The most prominent virion protein, S, makes a single pass through the membrane envelope, with almost the entire molecule forming an amino-terminal ectodomain. Multimers of S make up the large peplomers, characteristic of coronaviruses that recognize cellular receptors and mediate fusion to host cells (Lai and Holmes, 2001).

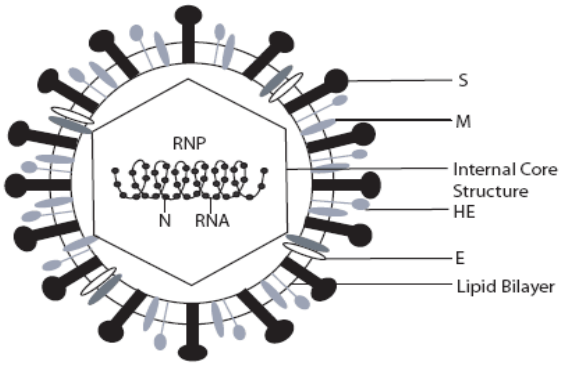

Figure 2 A model of typical coronavirus structure: S, spike glycoprotein; M, membrane glycoprotein; E, envelope protein; HE, hemagglutinin-esterase glycoprotein; N, nucleocapsid phosphoprotein; RNP, ribonucleoprotein.

Source: Lai and Holmes (2001)

Viral Genome

Genomic RNA of FCoV is positive-sense single-stranded, capped and polyadenylated (Rottier, 1999). They can function as mRNAs and the purified genomic RNA is infectious. At the 5'-end of the genome is the leader sequence RNA, which is present at the 5'-ends of all subgenomic mRNAs (Ruey -Yi *et al.*, 1994). Further downstream from the leader sequence is an untranslated region (UTR) of 200 to 400 nucleotides and at the 3'-end of the RNA genome contains another UTR of 200 to 500 nucleotides, followed by poly(A) of variable length (Lai and Holmes, 2001). Both the 3'- and 5'-UTR are important for RNA replication and transcription (Yi-Jyun *et al.*, 1994). Further downstream from 5'-UTR is the ORF which encodes the polymerase (Pol). It consists of two overlapping ORFs (1a and 1b) (Rottier, 1999). These ORFs are translated into a polyprotein, which is the precursor of viral polymerase. It is in part generated by ribosomal frameshifting and processed by proteolytic cleavages to generate the functional protein (Rottier, 1999). Further downstream from the polymerase gene is ORFs of genes for four structural proteins that are present in all coronavirus and

genes of largely unknown function. The organization of FCoV genome is 5'-Pol-S-E-M-N-3' (Rottier, 1999). Some coronavirus have a gene encoding the hemagglutinin-esterase (HE) glycoprotein located between Pol and S (Ruey -Yi *et al*., 1994).

S gene encodes peplomer or spike (S) glycoprotein (Herrewegh *et al*., 1995). The coronavirus S glycoprotein is a 180 to 200 kD molecule that is cotranslationally glycosylated in the endoplasmic reticulum (Gallagher *et al*., 1991). Most of the S population is then oligomerized into a trimeric structure. These S oligomers are transported toward the Golgi, where a large portion becomes incorporated into virions before budding into pre-Golgi vesicles (Gallagher *et al*., 1991). S glycoprotein then continues through the exocytic pathway. During virus maturation the S protein precursor is cleaved by a host cell protease which recognizes a basic sequence located approximately in the middle of the polypeptide (Routledge *et al*., 1991) into two subunits of similar-size, an amino-terminal half S1 and a carboxy-terminal half S2 (Gallagher *et al*., 1990). S1 and S2 are thought to correspond to the glubular and stalk regions, respectively, of the spike (Godet *et al*., 1994). All S glycoproteins posses' hydrophobic domains located at the terminal of the linear amino acid sequence (Gallagher *et al*., 1991). Cleavage of the spike occurs in many but not all coronaviruses. Some coronavirus in group I (eg. FIPV and BCoV) mature without cleavage of S protein (Hingley et al., 1998; Gombold et al., 1993). The S1 subdomain contains sequences that are responsible for binding to specific receptors on the membranes of susceptible cells (Hingley et al., 1998; Gombold et al., 1993). S1 sequences are variable, containing various degrees of deletion and substitutions in different coronavirus strains or isolates. Mutation in S1 sequences have been associated with altered antigenicity and pathogenicity of the virus (Hingley et al., 1998; Godet *et al*., 1994; Gombold et al., 1993; Lai and Holmes, 2001). In contrast, S2 sequences are more conserved (Lai and Holmes, 2001). Some of the S proteins which are not assembled into virions are transported by the secretory system to the cell surface where they are free to interact with adjacent cell, resulting in cell fusion (syncytia) (Gombold et al., 1993).

M gene encodes a matrix glycoprotein (M). E gene encodes a small envelope protein which is associated with the viral envelope. Both E and M proteins are required for budding of virions. Finally N gene encodes the nucleocapsid protein associated with genomic RNA to form ribonucleoprotein. These proteins are present in all coronaviruses (Hohdatsu *et al*., 1998 b; Rottier, 1999).

Feline Coronavirus Replication

1. Attachment

Attachment is the first step in the viral replication cycle, the binding of virions to the plasma membranes of target cells. Coronavirus entry starts with viral and cellular membrane fusion which is mediated by the binding of the viral S protein with cellular receptors (Lai and Holmes, 2001).

Coronavirus are group of enveloped, positive-strand RNA viruses. The envelopes of coronaviruses contain a spike protein (S), which binds to receptors on the target cell membrane. Some viruses in serogroup II have an additional hemagglutinin esterase, which binds to cell membrane molecules bearing 9-O-acetylated neuraminic acid (Lai and Holmes, 2001). Coronaviruses of serogroup I interact species-specifically with aminopeptidase-N (APN) as the attachment receptor (Hegyi and Kolb, 1998). APN is a 150 kD glycoprotein with metalloprotease activity (Tresnan *et al*., 1996). It is a type II transmembrane glycoprotein and belongs to the family of membrane-bound metallopeptidases, also called CD13 antigen. The protein is expressed on the plasma membranes of cells of granulocyte and monocyte lineages, as well as on nonhematopoetic tissues including fibroblasts, endothelial cells, synaptic membranes in the central nervous system (CNS), epithelial cells from the renal proximal tubules and intestinal brush border and epithelial cells of the respiratory tract (Tresnan *et al*., 1996). The physiological functions of APN differ depending on cell type. In the intestinal brush

border membrane, APN cleaves N-terminal amino acid of small peptides in the final steps of digestion and helps absorption of peptides from the small intestine (Hohdatsu *et al*., 1998 b). Feline aminopeptidase N (fAPN) is a receptor for FCoV, FECV and type II FIPV but not for type I FIPV (Hohdatsu *et al*., 1998 b). The amino acid sequences of S proteins of type I and type II FIPVs showed only about 46% homology (Motokawa, 1996), which may have been responsible for the differences in binding to the receptor between these FIPVs.

Human APN (hAPN) is a receptor for HCoV-229E and porcine APN (pAPN) is a receptor for TGEV and PRCV. Although hAPN and pAPN have a sequence similarity of 78% at amino acid level, HCoV-229E cannot utilize pAPN as a receptor and TGEV cannot utilize hAPN as a receptor. In contrast, feline APN (fAPN) does not display this species specificity in that it serves as a receptor not only for FIPV and FECV but also for TGEV, HCoV-229E and CCoV (Hegyi and Kolb, 1998; Tresnan *et al*., 1996).

2. Penetration and Uncoating

After virion binds to specific receptors on host cell, the specificity of virus-receptor interactions frequently determines which cell, tissue and species are susceptible to virus infection. On binding to its specific receptor under optimal conditions of pH and temperature, the viral attachment glycoprotein undergoes one or more programmed conformational changes that expose a hydrophobic fusion peptide which mediates fusion of the viral envelope with host cell membranes, releasing the viral nucleocapsid into the cytoplasm (Sturman *et al*., 1990; Zelus *et al*., 2003). Conformational changes in spike glycoprotein of some enveloped RNA virus is pH-independent fusion. The pH-independent fusion occurs when the viral envelope can fuse directly with the plasma membrane at neutral pH (Zelus *et al*., 2003). The pH-independent viruses cause cell-to-cell fusion, forming multinucleated syncytia in infected cell cultures and tissues when viral spike protein expressed on the membrane

of a cell are triggered to undergo a fusion-inducing conformational change by binding to a specific virus receptor on an adjacent cell (Zelus *et al*., 2003). Some enveloped RNA viruses, the spike glycoprotein require an acidic environment to trigger the conformational changes in the viral fusion protein that lead to membrane fusion (Sturman *et al*., 1990). Therefore, fusion of these viral envelopes occurs not at the plasma membrane but within the cell at endosomal membranes once the pH drops to 5.5. These pH-dependent or acid-dependent viruses do not induce the formation of multinucleated syncytia in cells and tissues at neutral pH (Zelus *et al*., 2003). Coronaviruses can enter cells either by pH-dependent endocytosis or by pH-independent fusion at the plasma membrane (Lai and Holmes, 2001). A coronavirus mouse hepatitis virus (MHV) causes cell fusion in intestinal epithelial cells during infection *in vivo* in the alkaline environment of the small intestine (Sturman *et al*., 1990). Infection of susceptible murine cells with the MHV type 4, results in extensive cell-cell fusion at pH from 5.5 to 8.5 (Gallagher *et al*., 1991). The mechanism of virus uncoats and releases its genomic RNA into cytoplasm is not yet clear. Cellular factors may be required for both virus penetration and uncoating (Lai and Holmes, 2001).

3. Transcription

Coronavirus is enveloped virus containing a large position-sense single-strand RNA. The viral genome is translated only to produce the polymerase polyprotein(s). Expression of the other genes requires the synthesis of five to seven subgenomic mRNAs (An *et al*., 1998; Yokomori *et al*., 1992). These viral mRNAs are represented by numbers in order of decreasing size. The mRNAs discovered after these assigned numbers are denoted by a hyphen and a second number (e.g. mRNA 2-1). The viral RNA is released into cytoplasm. It is used to synthesize a viral RNA-dependent RNA polymerase, which then initiates the transcription of viral mRNAs. Cells infected with coronavirus produce five to seven subgenomic viral mRNAs, depending on the coronavirus strain or isolate, each of which translates one or, occasionally, more than

one protein (Lai and Holmes, 2001). Coronavirus-infected cells contain multiple overlapping subgenomic, capped and polyadenylated mRNAs (Stohlman *et al.,* 1988). These mRNA have a 3'-coterminal nested-set structure; i.e., the sequence of each mRNA starts from the 3'-end of genome, extending for various distances into the 5'-end and is contained entirely with in the next-larger mRNA (Yokomori *et al*., 1992). Although each mRNA, except the smallest, contains two or more ORFs, only the 5'-most ORFs which contain the unique sequence not overlapping with the sequence of the next-smaller mRNA is translated (Yokomori *et al*., 1992). Thus, these mRNAs are functionally monocistronic. The 5'-end of each coronavirus genomic RNA and subgenomic mRNA starts with a leader sequence that is approximately 60 to 90 nucleotides (nt) long (An *et al*., 1998; Yokomori *et al*., 1992). This leader sequence is not found elsewhere in the genome; however, the sequence between each gene, termed the intergenic sequence, or transcription-associated sequence (TAS), shares a sequence homology of 7 to 18 nucleotides with the 3' end of the leader (Yokomori *et al*., 1992; Lai and Holmes, 2001). These intergenic regions are the fusion sites between the leader RNA and the rest of sequences in each mRNA and represent the transcription initiation sites for each mRNA (Yokomori *et al*., 1992).

According to the currently accepted model for discontinuous, leader-primed transcription of coronavirus RNA (Jeong and Makino, 1994; Lai and Holmes, 2001). According to this model, discontinuous transcription occurs during positive-stranded RNA synthesis. The genomic RNA is first transcribed into a full-length negative-stranded RNA. Transcription of the leader RNA begins at the 3'-end of the full-length, negative-stranded template RNA and terminates at the end of the leader sequence. The leader RNA becomes separated from its negative-sense template while remaining bound to polymerase. The leader-polymerase complex may then reattach to the template further downstream at one of the noncoding intergenic regions separating the various ORFs. Each intergenic region contains a short sequence called an intergenic sequence (IS) that is complementary to a portion of leader RNA. The IS could bind to the polymerase-

leader RNA complex and initiate mRNA synthesis, resulting in an mRNA that contains a leader RNA fused to the mRNA (Lai and Holmes, 2001). Several pieces of evidence are consistent with this model. Studies using ultraviolet (UV) light transcriptional mapping showed that synthesis of a genomic-sized RNA is a prerequisite for subgenomic mRNA transcription. The viral genomic RNA is first transcribed into negative-stranded RNA, which is then used as the template for synthesis of mRNAs and genomic RNA (Yokomori *et al*., 1992).

MHV-infected cells contain free leader RNAs ranging in size from 50 to 90 nucleotides (Lai and Holmes, 2001). There are different components involved in the regulation of MHV mRNA transcription (Zhang *et al*., 1994). The IS has been recognized in numerous analyses of mRNA transcription of coronavirus. The 3'-end of the MHV leader sequence consists of two to four copies of a pentanucleotide sequence (UCUAA), while IS preceding each viral gene includes a consensus UCUAAAC or similar sequence (Most et al., 1994; Zhang *et al*., 1994). The fusion of the leader sequence with the mRNA body sequence occurs between the UCUAA repeats of the leader and the consensus IS (Most et al., 1994). Site-specific mutagenesis and deletion studies have further defined the sequence requirement of this region for transcription (Joo and Makino, 1992). The *trans*-acting leader RNA, the sequence of the leader RNA, affects in *trans* the transcription efficiency of certain mRNA species. Leader RNAs transcribed from two different MHV strains in the same cell can be randomly joined to mRNAs from both strains (Lai and Holmes, 2001). The *cis*-acting leader RNA, MHV mRNA 2-1, can be transcribed only when the leader RNA sequence (particular its 3'-end) and the IS proceeding the gene are compatible (Liao and Lai, 1994; Lai and Holmes, 2001). Studies using a gel mobility shift assay showed that the MHV N protein binds not only to the positive-stranded genomic-length RNA but also to all six subgenomic mRNA. The specific interaction occurs between the N protein and sequences with in the leader RNA which is conserved at the 5'-end of all MHV RNAs (Stohlman *et al*., 1988).

4. Replication of Genomic RNA

Coronaviruses possess a positive-strand polyadenylated RNA genome that undergoes replication entirely within the cytoplasm of infected cells (Chang et al., 1994). During coronavirus replication, a minus-strand copy of the full-length genome (the anti-genome) and minus-strand counterparts of the six to eight 3'-coterminal subgenomic mRNAs are generated (Chang et al., 1994). Minus-strand RNA synthesis represents the first step in the synthesis of various RNA species in the replication cycle of positive-strand RNA viruses (Lin et al., 1994). Minus-strand RNA is used as a template to synthesize genomic RNA and mRNAs during viral replication (Lin et al., 1994). Unlike the discontinuous synthesis of subgenomic mRNA, the genomic RNA replication is presumably synthesized from a genomic-length minus-strand RNA template by a continuous replication process (Lin et al., 1994; Lai and Holmes, 2001).

5. Translation of Viral Proteins

Coronavirus mRNAs contain multiple ORFs, but only the 5'-most ORF of each mRNA is generally translated by a cap-dependent ribosomal scanning mechanism. It was found that a 5' leader sequence upstream of each mRNA enhances translation in virus-infected cell lysates (Lai and Holmes, 2001; Rottier, 1999). The structural protein, including S, M, N and HE, are translated from different mRNAs by this mechanism. Other viral proteins are translated by other distinct mechanisms. The mRNA1 of coronavirus contains two large overlapping ORFs, encoding polymerase, which is translated into one polyprotein by a ribosomal frameshifting mechanism (Lai and Holmes, 2001). The polyprotein, precursor protein, is processed by proteolytic cleavages to generate the functional proteins (Rottier, 1999). Some coronavirus mRNAs encode more than one different polypeptide from an individual ORF. It has been proposed that the expression of the distal regions of the ORFs is mediated by a leaky-scanning mechanism. The third ORF of IBV mRNA3, are preceded by an internal

ribosomal entry site sequence that allows ribosomes to bypass the upstream ORFs and translate the downstream ORF (Liu and Inglis, 1992).

6. Assembly of Virions

Coronaviruses contain at least three structural proteins: nucleocapsid (N) phosphoprotein associated with the genomic RNA, membrane glycoprotein (M) largely embedded within the lipid membrane and spike glycoprotein (S) which forming the petal-shaped spikes which protrude from the virion envelope (Delmas and Laude, 1990). Both glycoproteins are synthesized on ribosome bound to the rough endoplasmic reticulum (RER) (Vennema *et al*., 1990). Coronaviruses are assembled intracellular at membranes of the intermediate compartment, between the ER and Golgi apparatus (Vennema *et al*., 1996). The helical nucleocapsids which are synthesized in the cytoplasm align at these membranes and probably interact with the cytoplasmic domain of viral membrane proteins. They are incorporated into viral particles by budding (Vennema *et al*., 1996).

The first step in virus assembly is the binding of N protein to viral RNA to form helical nucleocapsids in cytoplasm. MHV nonstructural proteins, including RNA polymerase and RNA proteinase, are translated from MHV-specific genomic-sized mRNA1 (Woo *et al*., 1997). This mRNA interacts with the nucleocapsid protein to form a helical nucleocapsid structure (Stohlman *et al*., 1988). Other MHV structural and nonstructural proteins are synthesized from six to seven smaller species of subgenomic mRNAs, mRNA2 to mRNA7. Only mRNA1 is packaged into MHV virions (Woo *et al*., 1997). A 69 nucleotide long RNA necessary for RNA packaging so called packaging signal is identified within Defective interfering (DI) RNAs of MHV (Woo *et al*., 1997). This packaging signal resides at about 20 kb from the 5'-end of the MHV genome and presumably is necessary for packaging of MHV mRNA1 into MHV particles (Woo *et al*., 1997). This sequence, found only in the genomic-length RNA, specifically binds the N protein (Masters *et al*., 1994). The packaging signal forms a stable stem-loop structure

important for its biological function (Woo *et al*., 1997). All seven MHV mRNAs are associated with the MHV nucleocapsid protein. A specific interaction occurs between the MHV nucleocapsid protein and the sequence resigned with in the leader RNA. The packaging signal sequence is conserved at the 5'-end of all MHV RNAs (Stohlman et al., 1988). BCoV, TGEV and IBV virions also incorporate small amounts of all subgenomic mRNAs which do not contain the packaging signal (Hofmann *et al*., 1990; Sethna *et al*., 1989 and 1991).

Once the nucleocapsid is formed, it interacts with the M protein at the cellular membranes. M protein is the most abundant protein which spans the membrane bilayer three times with extending of the NH_2-terminal domain outside the virion (or exposed luminally in intracellular membranes) and the COOH terminus (cytoplasmic domain) inside the virion (Haan *et al*., 1998). The main function of M protein involves the organization of viral envelope and the interaction with the nucleocapsid during assembly (Godkye et al., 2000). MHV M protein accumulates in the Golgi apparatus and is believed to determine the site of budding (Klumperman *et al*., 1994). The M protein is inserted in ER and anchored in the Golgi apparatus. The nucleocapsid is incorporated into a viral particle by budding into the intermediate compartment between the ER and Golgi apparatus (Haan *et al*., 1998). MHV M protein Interacts with viral nucleocapsid by a temperature-dependent conformational change of M protein, resulting in aggregation of M protein and interaction with the viral ribonucleoprotein (Sturman *et al*., 1980).

Another component essential in the assembly process is the envelope protein (E) (Godkye et al., 2000). E protein is also transported through the ER to the Golgi apparatus, where E and M proteins interact to trigger the budding of virions and enclosing the nucleocapsid (Lai and Holmes, 2001). The spike glycoprotein (S) has been shown to mediate attachment of virions to the host cell receptor, involve in cell-to-cell fusion, induce neutralizing antibodies and bear virulence determinants. During its biosynthesis, the S polypeptide is co-translationally N glycosylated, in which the

carbohydrates are processed in the ER and in the Golgi apparatus (Delmas and Laude, 1990). For several coronaviruses, posttranslational event of S gene is the proteolytic cleavage into two polypeptides, S1 and S2 (Delmas and Laude, 1990). A proportion of S protein which is not incorporated into virions is transported to the plasma membrane (cell surface), where it induces cell-to-cell fusion (Vennema *et al*., 1990). Upon transported to Golgi apparatus, S protein interacts with M protein and are incorporated into the maturing virus particles (Vennema *et al*., 1996). Coronavirus assembly is not dependent on the S protein. Virus-like particles (VLPs) can be assembled from the M and E proteins by simple co-expression of their genes within cells in which neither the S protein nor a nucleocapsid is required (Godkye et al., 2000).

7. Budding of Virions

MHV budding is first detectable by electron microscopy at 6 to 7 hours post infection in perinuclear vesicles and tubules in a region transitional between the RER and the Golgi apparatus (Tooze *et al*., 1984). M protein is confined at 6 hours post infection to the perinuclear region while at later times it also accumulates in the ER. At 6 hours post infection the S protein is distributed throughout the ER and is not restricted to the site at which budding begins (Tooze *et al*., 1984). The ratio of M to E protein in virions can be as high as 100:1 (Vennema *et al*., 1996). The time and the site for maturation of progeny virions are determined by the accumulation of M protein in intracellular membranes. Budding never occurs on the plasma membrane probably because the M protein is never found on the plasma membrane (Tooze *et al*., 1984). After budding virus particles may undergo further morphologic changes within the Golgi apparatus, resulting in the appearance of mature virus particles with a compact M protein.

Feline Enteric Coronavirus Infection

FECVs cause mild intestinal infections in kittens between the fifth to the twelfth weeks of age. FECV are antigenically and morphologically similar to FIPV (Vennema *et al*., 1998). The particle is virtually indistinguishable from FIPV (Hoshino and Scott, 1980; Pedersen *et al*., 1981). Serum antibodies to the enteric coronavirus cross-react indirect fluorescent antibody, ELISA and virus neutralization test with FIPV, CCoV and TGEV (Pedersen *et al*., 1981). The major difference between FECV and FIPV isolates is that FECV is unable to cause FIP. The first isolate, designated FECV-UCD has not been propageted in tissue culture. This strain produces mild or unapparent enteritis in specific pathogen-free cats (Pedersen *et al*., 1984). A second isolate, FECV-79-1683, was isolated from a fatal case of peracute hemorrhagic enteritis in an adult cat. This strain replicates in tissue culture and produces a cytopathic effect similar to that of CCV (Pedersen *et al*., 1984). The FECV infection is present within most catteries and multiple-cat householdes (Pedersen *et al*., 1981), indicating that these types of environment are more conducive to disease. Approximately 80 to 90 percent of the cats within individual catteries and multiple-cat householdes can be seropositive (Pedersen, 1995). The infection may recur throughout life in some cats and is manifested by waxing and waning of the coronavirus titers at intervals of several months to several years (Pedersen *et al*., 1984).

1. Pathogenesis

The major source of virus appears to be asymptomatic carrier cats that shed FECV in their feces (Pedersen *et al*., 1984). The pathogenesis of FECV infection is similar to that of CCoV and TGEV infection (Pedersen *et al*., 1984). As in the porcine and canine diseases, enteritis occurs mainly in young animals. Kittens become infected between the fifth and twelfth week of age (Pedersen, 1995). Systemic passive immunity as well as lactogenic immunity may play some role in delaying infection until kittens reach weaning age. The queens pass on IgG antibodies in their colostrum (Pedersen *et*

al., 1984) and presumably IgA antibodies in their milk. These antibodies appear to have a protective function because kittens are not usually infected until some time between the fifth to twelfth weeks of age. With early infection, the virus is found in the saliva, urine and respiratory secretions, but later on it remains in the feces only. The major target tissue for the virus is the mature apical epithelium of the intestinal villi. FECV-79-1683 was found at the highest concentration in the ileum, jejunum, duodenum and mesenteric lymph nodes, while intermediate amounts of virus were found in the cecum, tonsils and thymus (Pedersen *et al*., 1984). Virus shedding in the feces peaked about seven days after oronasal infection (Pedersen *et al*., 1984). Infection occurs when carrier and susceptible cats are placed in contact with each other (Pedersen *et al*., 1981 and 1984). Infection can also spread when dirty litter pans are interchanged between rooms containing carrier and susceptible cats.

2. Clinical Signs

The disease in cattery-reared kittens is often inapparent. A mild or moderately sever diarrhea may persist for two to five days in some cats (Addie and Green, 1998). The severity of the disease in specific pathogen-free kittens is somewhat age-dependent (Addie and Green, 1998). The fifth-week old kittens that are infected orally frequently develop clinical disease. The illness varies from moderately sever to inapparent depending on the individual (Addie and Green, 1998). The infection in the twelfth-week-old kittens is mild or inapparent but in adult cats is usually inapparent (Addie and Green, 1998). Clinical disease is manifested by a low-grade fever beginning on the third to sixth day after infection. Just before fever develops, bowel movement may become more frequent and there may be intermittent vomiting (Pedersen *et al*., 1984). Within a day or so the stools become progressively more fluid and mucus-laden. Fresh blood sometimes appears in the stool (Pedersen *et al*., 1984).

Lesions are more likely to be observed in the jejunum and ileum than the duodenum (Addie and Green, 1998). Histopathologic changes are also present to varying degrees, but are generally mild. In severe cases, the infection tends to be patchy throughout the length of the involved intestine. Microscopically, lesions evolve as follows: vacuolation and syncytium formation of the mature epithelial cells on the tips of the intestinal villi; fusion of adjacent villi; sloughing of the infected epithelium of the apical portion of the villi and hyperplasia of the crypt epithelium (Pedersen *et al*., 1981).

Feline Infectious Peritonitis Virus Infection

Feline infectious peritonitis virus (FIPV), a mutant of FECV, infects domestic and wild feline of all species (Venema *et al*., 1998). As other coronaviruses, the virions are 90-120 nm in diameter, with 15 nm petal-shaped envelope projections called peplomers (Hoshino and Scott, 1980). FIPV causes a fatal systemic disease of feline, called feline infectious peritonitis (FIP). FIP is an immune complex-mediate disease of domestic and wild feline. There are two different forms of the disease. The first, effusive or wet, form is characterized by peritonitis or pleuritis or both. The second form, noneffusive or dry form is characterized by granulomas in various parenchymatous organs (Ficus *et al*., 1987). FIPV is found mainly in macrophages, where it replicates and buds from internal profiles of ER (Pedersen, 1976). Virus is shed in feces and may replicate in the tonsils and oropharynx and is also shed in the saliva (Pedersen, 1995). The virus is relatively unstable outside the body, ether- and heat-labile and very susceptible to most commonly used disinfectant (Pedersen, 1976).

FIPV was first propageted *in vitro* in peritoneal macrophage cultures (Pedersen, 1976) and later in whole-organ ring cultures of intestine and trachea and primary cultures of feline fetal cells (Hoshino and Scott, 1980). It has also been adapted to grow in the brains of sucking mice, rats and hamsters (Horzinek and Osterhaus, 1979; Pedersen, 1976). At least six FIPV isolates have been cultivated in tissue culture: FIPV-UCD1, FIPV-UCD2, FIPV-UCD4, FIPV-DF2, FIPV-TN406 and FIPV-79-1146 (Ficus and

Teramoto, 1987). Some strain, such as FIPV-TH406 and FIPV-79-1146, are highly infectious and most infected cats develop FIP (Table 3) (Ficus and Teramoto, 1987).

FIPV isolates were divided into two distinct antigenic groups with monoclonal antibodies (MAb) library. One antigenic group included the more virulent FIPV isolates, whereas an avirulent isolate, FIPV-UCD2, was the sole member of the second antigenic group (Ficus *et al*., 1987). In general, MAb directed to E glycoprotein and N protein recognized all of the FIPV isolates. The antigenic sites of this structural polypeptide are highly conserved (Ficus *et al*., 1987). In contrast, other MAbs were used to differentiate the S glycoprotein of virulent and avirulent FIPV (Ficus and Teramoto, 1987). FCoV type II strain FCoV-79-1683 and FIPV-79-1146 originated from a double recombination between FCoV type I and CCoV. Comparative sequence analysis of genomic region in *pol* gene of FCoV type I strains (FIPV-UCD1 and FIPV-TN406), FCoV type II strains (FIPV-79-1146 and FCoV-79-1683) and CCoV strain, show that the FCoV type II have arisen from double recombination event: additional crossover sites were mapped in the ORF1ab frameshifting region of FCoV-79-1683 and in the 5'-half of ORF1b of FIPV-79-1146 (Herrewegh *et al*., 1998).

1. Pathogenesis

FIP is an immune complex disease involving viral antigens, antiviral antibodies and complement. Complement fixation leads to the release of vasoactive amines, which cause endothelial cell retraction and thus increased vascular permeability. Retraction of capillary endothelial cells allows exudation of plasma protein, which is the characteristic protein-rich exudate developed in effusive FIP (Flint *et al*., 2000). Neutrophils pass through the gaps between the endothelial cells and release lysosomal enzymes, causing necrosis of the vessel wall. The neutrophil is the characteristic cell type encountered in FIP granulomas (no effusive from) (Flint *et al*., 2000).

Table 3 Feline infectious peritonitis virus isolates

Isolate	Source	FIP pathogenicity
FIPV-UCD1	Pedersen,University of California, Davis	++
FIPV-UCD2	Pedersen,University of California, Davis	-
FIPV-UCD4	Pedersen,University of California, Davis	+
FIPV-DF2	American Type Culture Collection, Rockville, MD.	++
FIPV-TN406	Black, Specialized Assays, Nashville, Tenn.	++
FIPV-79-1146	Evermann, Washington State University, Pullman	++

Note -, has never been shown to cause FIP in experimental cats; +, sometimes causes FIP in experimental cats; ++, usually causes FIP in experimental cats.

Source: Ficus and Teramoto (1987)

Domestic cat and other *Felidae*, including lions, mountain lions, leopards, jaguars, cheetahs, lynxes, sand cats and pallas cats, are susceptible to infection with FIPV (Pedersen, 1995). In domestic cats, FIP disease occurs predominantly in young animals, although all ages are susceptible. A higher incidence occurs between the sixth and twelfth months of age, whereas a lower incidence is noted from the fifth to thirteenth years of age, followed by an increased incidence in cats fourteenth years of age and older (Pedersen, 1995). Male and female cats are affected equally (Pedersen, 1995).

The natural route of FIPV infection is unknown although cats can be experimentally infected by oral, nasal and parenteral administration of virus. Following infection by these routes, FIPV first replicates in the epithelial cells of the upper respiratory tract or intestine (Figure 3) (Hohdatsu *et al*., 1998 b).

A primary viremia results in free virus and virus-infected epithelial cells being transported to other organs, especially to the liver, spleen and lymph nodes. These organs are subsequently involved because they contain large population of macrophages, which are the principal target cells for FIPV infection (Foley and Leutenegger, 2001). A secondary macrophage-associated viremia then occurs, resulting in further spread of FIPV throughout the body (Foley and Leutenegger, 2001). In an individual cat in which both FIPV and the correct predisposing factors are present, dissemination of the virus in macrophages will occur and FIP may develop. Clinically apparent FIP occurs after the viruses infect macrophages and monocytes and then cross the mucosal barrier and spread throughout the body of the cat (Hohdatsu *et al*., 1998 b). If an effective cell-mediated immune (CMI) response is exhibited during the primary phase of FIPV infection, viremia will probably be terminated, thereby protecting the cats against FIP disease (Foley and Leutenegger, 2001). If the infected cat is unable to mount an effective CMI response and produces antibodies that do not neutralize the virus, infection progresses rapidly into an effusive form of FIP disease (Figure 3) (Andrew, 2000). Cats with no anti-FCoV antibody do not developed FIP (Foley and Leutenegger, 2001).

There are two possible explanations for the events following viral dissemination from the upper respiratory tract or intestine. First, FIPV-infected macrophages leave the blood stream and enable virus to enter the tissue. The virus attracts antibodies, complement is fixed and more macrophages and neutrophile are attracted to the lesion. Noneffusive may be a result of a partially CMI response to contain the infection (Figure 3) (Andrew, 2000).

Alternatively, in cats that develop effusive FIP, there may be a large quantity of virus present, leading to the formation of great numbers of CICs (circulating immune complexes) and the destruction of many blood vessels. Noneffusive FIP may result from

the production of fewer CICs or of CICs that neither attaches to blood vessel walls nor fixes complement efficiently (Andrew, 2000).

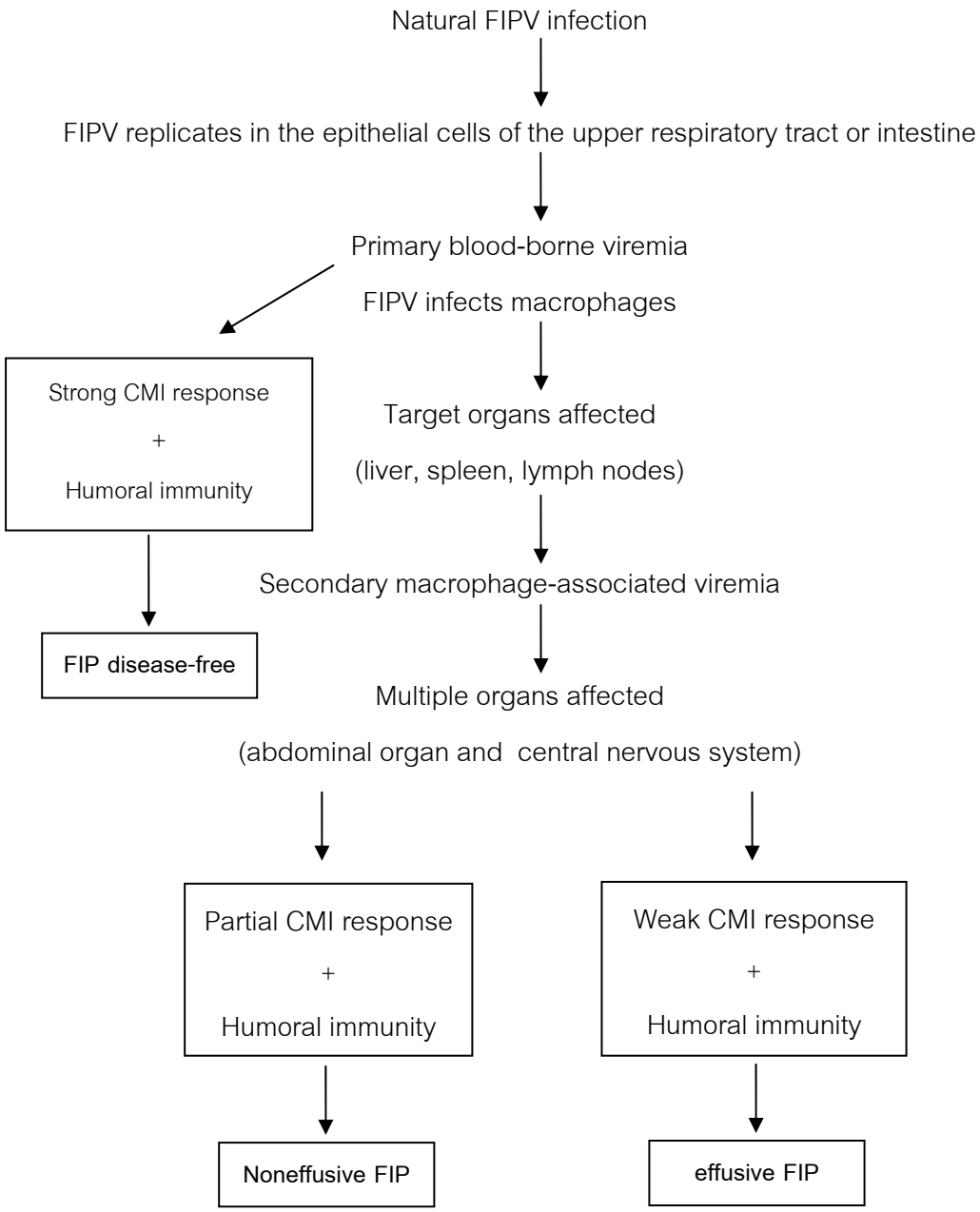

Figure 3 Pathogenesis of feline infectious peritonitis (FIP)

Source: Hoskins (1993)

The pathologic consequences of the formation of immune complexes *in vivo* depend on their sites, as well as antibody and antigen contents. Immune complex deposition is most likely the site of high blood pressure and turbulence and such condition occurs at blood vessel bifurcation (Andrew, 2000). FIP lesions are most common in the peritoneum, kidney and uvea, all of which are sites of high blood pressure and turbulence (Andrew, 2000). Effusive FIP is usually the more acute form of the disease (although it can occur terminally in cases of noneffusive FIP) (Foley and Leutenegger, 2001).

The pathogenesis of FIP is further complicated by the phenomenon of antibody-dependent enhancement (ADE) (Hohdatsu *et al*., 1998 a). Generally, macrophages play an important role in non-specific defense against viral infection. Some viruses bound to antibody invade macrophages via the Fc region of the antibody and the Fc gamma receptor (Fc γ R) of the macrophage and eventually the antibody leads to the enhancement of infection (Hohdatsu *et al*., 1998 a). The antibodies against FIPV facilitate the uptake of FIPV into macrophages. Thus, they enhance the FIPV infection and accelerate the disease onset in cats (Hohdatsu *et al*., 1998 a; Foley and Leutenegger, 2001). Cats with FIPV neutralizing antibody from previous natural exposure to virus or passive transfer of antibody frequently develop disease far more rapidly and more severely than cats that have not been previously exposed (Corapi et al., 1995; Hohdatsu *et al*., 1998 a). The enhancing effect of the antibody on FIPV infection impedes prophylaxis of FIP by vaccination (Hohdatsu *et al*., 1998 a). *In vitro* studies with neutralizing monoclonal antibodies (MAbs) to FIPV have shown that the major neutralizing epitope are confined to S glycoprotein and that they correspond, to a large degree, with the epitopes involved in ADE (Corapi et al., 1995).

2. Clinical Signs

The clinical and pathological signs that occur in FIP are a direct consequence of the vasculitis and the organ damage. Damage of the blood vessels causes leaking of the exudation of fluid and plasma proteins into the body cavities. The outcome of infection depends on the result of complex interaction among the strain and dose of virus, the route of infection and the age, genotype, immune competence and immune status of the cats (Pedersen, 1995; Hohdatsu *et al*., 1998 b). Clinical signs common in either the effusive or noneffusive forms of FIP disease include anorexia, weight loss, lethargy and mild pyrexia (39-39.5^{0}C) (Andrew, 2000).

Cats with effusive FIP have ascites (Figure 4-5). The amount of fluid varies from 25 to 700 ml or more (Savary *et al*., 2001). It is typically a nonseptic exudate of high total protein and low cellularity (i.e., total protein greater than 3.5g/dl; 1,000 to 2,000 nucleated cells/µl), consisting principally of nondegenerate neutrophils as well as lymphocytes and macrophages (Savary *et al*., 2001). With effusive FIP, the specific clinical signs depend on the body system affected by the vasculitis. Clinical signs can include combinations of any of the following: ascites causing abdominal distention with a fluid, thoracic effusion resulting in dyspnea, tachypnea and muffled heart sounds, scrotal enlargement, mucosal pallor or icterus, pericardial effusion, abdominal masses (adhesions) and mesenteric lymphadenopathy (Andrew, 2000). Cat with effusive cases tend to die within two months of the onset of clinical signs, whereas cats with noneffusive case have a more chronic disease course (Andrew, 2000).

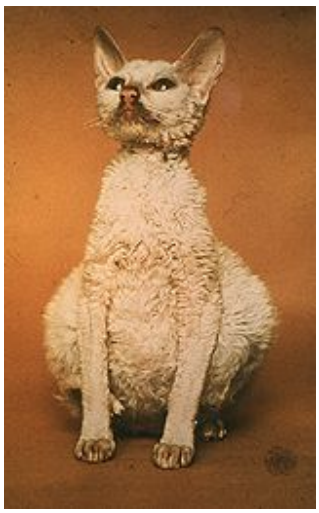

Figure 4 A pronounced case of effusive FIP form. The cat is emaciated with a pronounced extention of the abdomen.

Source: Horzinek and Lutz (2001)

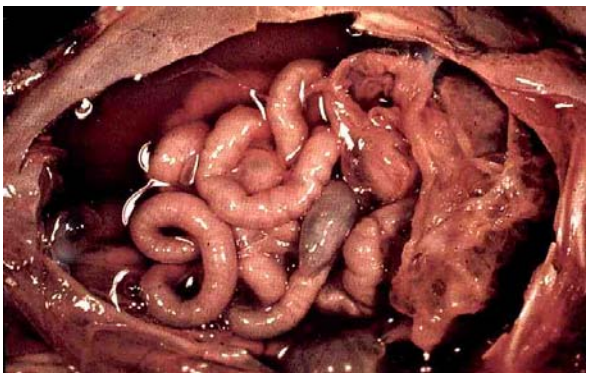

Figure 5 Abdominal cavity in effusive FIP. The abdomen is filled with a deep yellow, protein-rich exudate. The omentum is thickened and retracted into a compact mass behind the liver and stomach.

Source: Pedersen (2001)

Cats with noneffusive FIP are usually presented with a chronic fluctuating fever, malaise and weight loss extending over weeks or months (Andrew, 2000). This case may have granulomatous lesion in abdominal organs (spleen, kidney, liver and omentum), lungs and central nervous system (CNS) or eyes (Figure 6) (Andrew, 2000). Occasionally, granulomas are localized to the gastrointestinal tract, including the colon, ileocecocolic junction, or small intestine (Andrew, 2000). The abdominal lesions of effusive FIP are surface-oriented but extend into the parenchyma and range from less than 1 mm to 10 cm or more in diameter (Foley and Leutenegger, 2001).

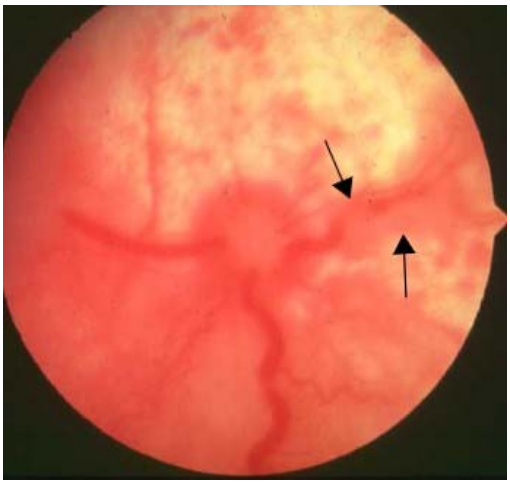

Figure 6 The retina of a cat with noneffusive FIP. The high protein exudate into the vitreous. Retinal blood vessels can be seen disappearing into pyogranulomata (arrow)

Source: Addie (2005)

3. Immunity

FIP is an immune-mediated, usually fatal disease of domestic and exotic felids. The disease presents as a fibrinous serositis, with accumulations of highly proteinaceous fluid within body cavities, disseminated pyogranulomata formation, hypergammaglobulinaemia and the formation of immune complexes. The pathogenesis of disease is complex, with CMI playing a protective role, while humoral responses are generally detrimental, aiding viral dissemination by opsonising its uptake by macrophages and resulting in immune complex formation (Andrew, 2000). The type and strength of immunity also determine the disease form (effusive or noneffusive). Cats with a strong CMI may not develop the disease, while those with a weak CMI have the noneffusive FIP (Paltrinieri *et al*., 1998). Effusive FIP occurs in cats that mount a humoral immune response but fail to develop concurrent protective CMI (Paltrinieri *et al*., 1998). Humoral immunity that enhances disease can also be generated by infecting cats with closely related strains of FECV, attenuated strains of virulent FIPV, or autologous and homologous low-virulence strains of FIPV (Pedersen, 1988). The humoral and cellular immunity in naturally occurring FIP found that in both effusive and noneffusive forms decreased albumin/globulin ratio with hypoalbuminemia, hyperglobulinemia and increased α_2-, β- and γ-globulins (Paltrinieri *et al*., 1998). The electrophoretic pattern of the effusions was always similar to that of the corresponding serum and antibody titers detected in the effusions were higher than those of the corresponding serum (Paltrinieri *et al*., 1998). In cellular foci of FIP lesions, many virus-infected macrophages and few lymphocytes were found. However, lymphocytes were more abundant when cellular foci and FIP-infected macrophages were centered around neoformed vessels (Paltrinieri *et al*., 1998). Cytokines are intimately involved in the control of immune reactions. During development of FIP, increased production of IL-6, IL-4 and IL-10 as well as reduced production of IL-2, IL-12 and/or IFN$_\gamma$ may result in decreasing protective CMI and increasing non-protective antibody response (Gunn-Moore *et al*., 1998; Dean *et al*., 2003). In 1996, Haagmans *et al*. have shown that the ascitic fluid from FIPV-infected

cats induces apoptosis in activated lymphocytes from uninfected cats, as does TNF-α (Haagmans *et al*., 1996). Two hypotheses have been proposed to explain failing to generate a protective cell-mediated response against FIPV. Apoptotic destruction of activated T-cells could undermine the cell-mediated response (Gunn-Moore *et al*., 1998). Secondly, humoral response observed in FIPV-infected cats and high IL-10: IL-12 ratios reduced production of IFN_{γ} (Gunn-Moore *et al*., 1998; Dean *et al*., 2003).

Diagnosis

A definitive diagnosis of FECV infection is difficult, because the clinical signs may be related to a number of other causes (Hoskins, 1993). Electron microscopy of feces to search for coronavirus particles is expensive, time-consuming and fraught with false-negative and false-positive results, though not routinely available (Hoskins, 1993). Although rising antibody titers to FCoV may indicate recent infection, interpretation of FCoV serology is problematic (Hoskins, 1993). Polymerase chain reaction (PCR) is available in some laboratories and may be used to detect FCoV in feces (Herrewegh *et al*., 1995).

A diagnosis of FIP can often be achieved through a combination of clinical and laboratory finding. A weighted scoring system has been described that can be used as an aid to clinical diagnosis (Table 4) (Pedersen, 1995). A score is given for each of the following factors and the total score is used to assess the likelihood that the cat has FIP. Cats scoring less than 75 are unlikely to have FIP; 75 to 200, FIP should be considered as a differential diagnosis; greater than 200, FIP should be at the top of the diagnostic list (Table 4) (Pedersen, 1995). Wet FIP is easier to diagnose than dry FIP because of the presence of fairly characteristic abdominal or pleural fluid. The fluid, which in FIP is typically straw colored and viscous, it has a high protein content, may froth on shaking and may clot if stored refrigerated (Greene, 1998). The protein content of the effusion is high because of the raised levels of gamma globulins (Greene, 1998). Clinical findings (fever, uveitis, neurological signs, or icterus) combined with historical factor (young cat,

multicat household or possible exposure to carrier animals and a recent stressful event) and laboratory findings (hyperglobulinemia (>5.1 g/dl) and lymphopenia (<1.5 x 10^3 cells/μL)) result in high predictive value (>85%) that will be diagnosed postmortem (Greene, 1998). Because virus isolation is difficult in FIP, serology has been used to aid diagnosis. However, serology does not distinguish between infections with harmless feline coronavirus (FECV) and virulent FIPV and can not distinguish between post and present infection (Herrewegh *et al*., 1995). In the absence of clinical signs, serology is of no use in determining prognosis. Serologic tests used for FIP are generally based on immunofluorescent antibody or ELISA-based techniques. However, antibody titers may vary among laboratories. Antibody titer of 1:400 to 1:25,600 was seen in cats with both effusive and noneffusive forms of FIP (Pedersen, 1976). PCR is a highly sensitive technique for amplifying and detecting small amounts of DNA. Because FCoV is an RNA virus, a DNA copy must first be made utilizing the enzyme reverse transcriptase. A nested reverse transcriptase PCR (RT-nPCR) can be performed to detect FCoV particles in tissue or fluid samples (Herrewegh *et al*., 1995). The RT-nPCR for detect FCoV particle was targeted to the 3'-UTR region that is highly conserved region of CCoV, TGEV and FCoV (Herrewegh *et al*., 1995). This technique is highly sensitive and specific for FCoV but can not distinguish between FECV and FIPV and the use for FIP diagnosis is limited because of the occurrence of apparently healthy FCoV carriers (Herrewegh *et al*., 1995).

In 1997, Gamble *et al*. developed a diagnostic test for FIPV infection based on a RT-nPCR assay (Gamble *et al*, 1997). The target for amplification is the sequence within S1 region of S gene that has sufficient sequence homology among FIPV strains but difference between FIPV and FECV (Gamble *et al*, 1997). This assay is able to differentiate FIPV from FECV. A dot blot hybridization assay, using a biotinylated cDNA probe, was able to detect FIPV in cell cultures (Martinez and Weiss, 1993). The probe cross-hybridized in the dot blot assay with nucleic acid of a closely related FCoV (Martinez and Weiss, 1993).

Table 4 A weighted scoring system for FIP diagnosis

Factors	Points
1. Antibiotic-resistant, persistent, spiking fever	10
2. Abdominal effusion	10
3. Pleural effusion	5
4. Above effusions yellowish, mucinous, high protein, fibrin tags; moderate numbers macrophages and polymorphonuclear neutrophil leukocytes	15 x sign 2 or 3
5. Icteric serum	5
6. Palpable or visual masses in mesentenric lymph nodes, kidneys, ileocecocolic area	5
7. Aspirates or biopsy of above masses shows granulomatous inflammation	15 x sign 6
8. Neurologic abnormalities	15
9. Anterior uveitis/retinitis	10
10. Anterior uveitis with keratitic precipitates	25
11. Characteristic complete blood count	10
12. Elevated serum globulin	10
13. Characteristic serum electrophoresis	15
14. FCoV antibody titer negative to 1:25	0
15. FCoV antibody titer 1:100 -1:400	5
16. FCoV antibody titer 1: 1600	10
17. FCoV antibody titer 1:3200 or greater	20
Total the above points and multiply by the following :	
a. The cat comes from a pure breed cattery or from a large multiple-cat environment (pound, shelter, pet store, multipet household)	3 x total points
b. The cat is from 3 months to 3 years of age	2 x total points

Source: Pedersen (1995)

MATERIALS AND METHODS

Virus and Clinical Specimens

1. FCoV and FIPV Reference Strains

The FCoV and FIPV reference strains were obtained from commercially available modified live intranasal FIP vaccine produced from temperature sensitive (ts) strain FIPV propagated on feline cell lines (Premucell FIP®).

2. Serum Samples

During May to September 2003, the serum samples were randomly collected from both solitary household cats and multicats households. These cats were either healthy or sick with clinical signs resemble FIP, from the central and eastern part of Thailand including Krung Thep Maha Nakhon, Pathum Thani, Nakhon Pathom, Ratchaburi, Suphan Buri, Samut Sakhon and Chon Buri. The sera were kept on ice during transportation and stored at -80°C until used. The positive FIPV controls (FIP12) were kindly provided by Dr. Panchit Nilkumhang of the Small Animal Hospital at Kasetsart University.

3. Case Definitions

The cats were defined as FIP cats if they presented the following clinical signs and findings. First, the sick cats showed clinical signs of abdominal and/or pleural fluid, uveitis and icterus. Secondly, laboratory findings of these cats included hyperproteinemia, hypergammaglobulinemia and albumin/globulin ratio less than 0.4. In addition, if there was no detectable fluid accumulation, the cats were further examined for the granulomatous lesions in mesenteric lymph nodes and other abdominal organs such as kidney and intestine by X-ray or ultrasound.

Primer Selection

The oligonucleotide primers for the detection of FCoV, sequence were obtained from the highly conserved 3'-UTR of FCoV genome. The sequences of the outer primers are FIP205 5'-GGCAACCCGATGTTTAAAACTGG-3' located between nucleotides 1 and 23 and FIP211 5'-CACTAGATCCAGACGTTAGCTC-3' spanning nucleotides 211 to 192. The internal primers include FIPg276 5'-CCGAGGAATTACTGGTCATCGCG-3' located from nucleotides 29 to 51 and FIPg204 5'-GCTCTTCCATTGTTGGCTCGTC-3' which is between nucleotides 205 to 184 (Figure 7) (Arnold *et al.,* 1995).

The target sequences of FIPV were chosen on the basis of mismatches with other related sequences, G+C content and melting temperature, corresponding to nucleotides 251 to 601, which are 69 bp upstream from the transcription start codon of the peplomer S gene. These primers consist of outer primers: FIP251 5'-CTACAGAGGTGTGGTACAAC-3' located between nucleotides 251 and 271 and FIP621 5'-TTCCACTCAAGACCATAGAT-3' spanning nucleotides 621 to 601. The internal primers include FIPs361 5'-GGTAATGCACGTGGTAAACC-3' located from nucleotides 361 to 381 and FIPs530 5'-CACTGGTTGGAGGTGAATTG-3' which are between nucleotides 530 to 510 (Figure 7) (David *et al.,* 1997).

RNA Extraction

Genomic RNA was extracted form the sera and effusive fluids of cats, using the RNeasy Total RNA Kit (Qiagen GmbH Germany) according to the manufacturer's instruction with slightly modification. Serum samples were first lyses and homogenized in the presence of a highly denaturing guanidine isothiocyanate (GITC) – containing buffer, which immediately inactivates RNases. After homogenization, 20 ng of poly-C RNA were added to the lysate as the carrier RNA. Ethanol was added to provide appropriate binding condition and the sample was then applied on to an RNeasy mini

column where the total RNA bound to the membrane and contaminants were efficiently washed away. RNA was then eluted by RNase-free water (Figure 8).

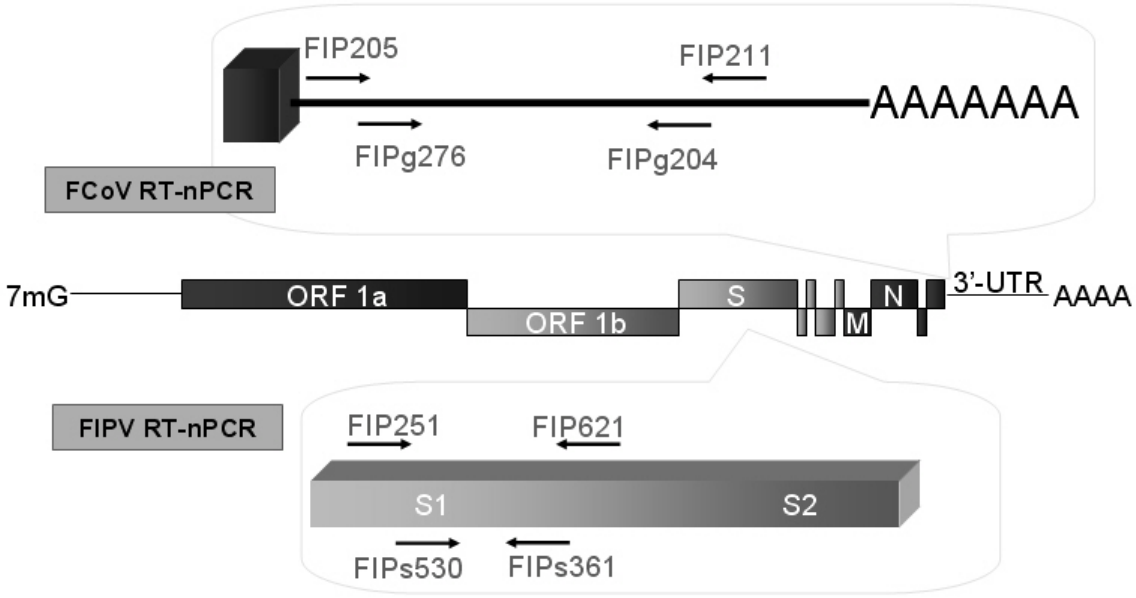

Figure 7 Positions of the selected primers for the RT-nPCR. The genomic RNA of FCoV is flanked with 7mG and poly A tail. Each gene of FCoV genes are represented by boxes, including the genes for polymerase (ORF 1a and ORF 1b), the spike protein (S), the membrane protein (M) and the nucleocapsid protein (N). The upper part shows the positions of the outer primers (FIP205 and FIP211) and the internal primers (FIPg276 and FIPg204) within the 3'-UTR region. In the lower part shows the position of the outer primers (FIP251 and FIP621) and the internal primers (FIPs530 and FIPs361) with in the S gene. Arrows indicate the 5'-to-3' orientations.

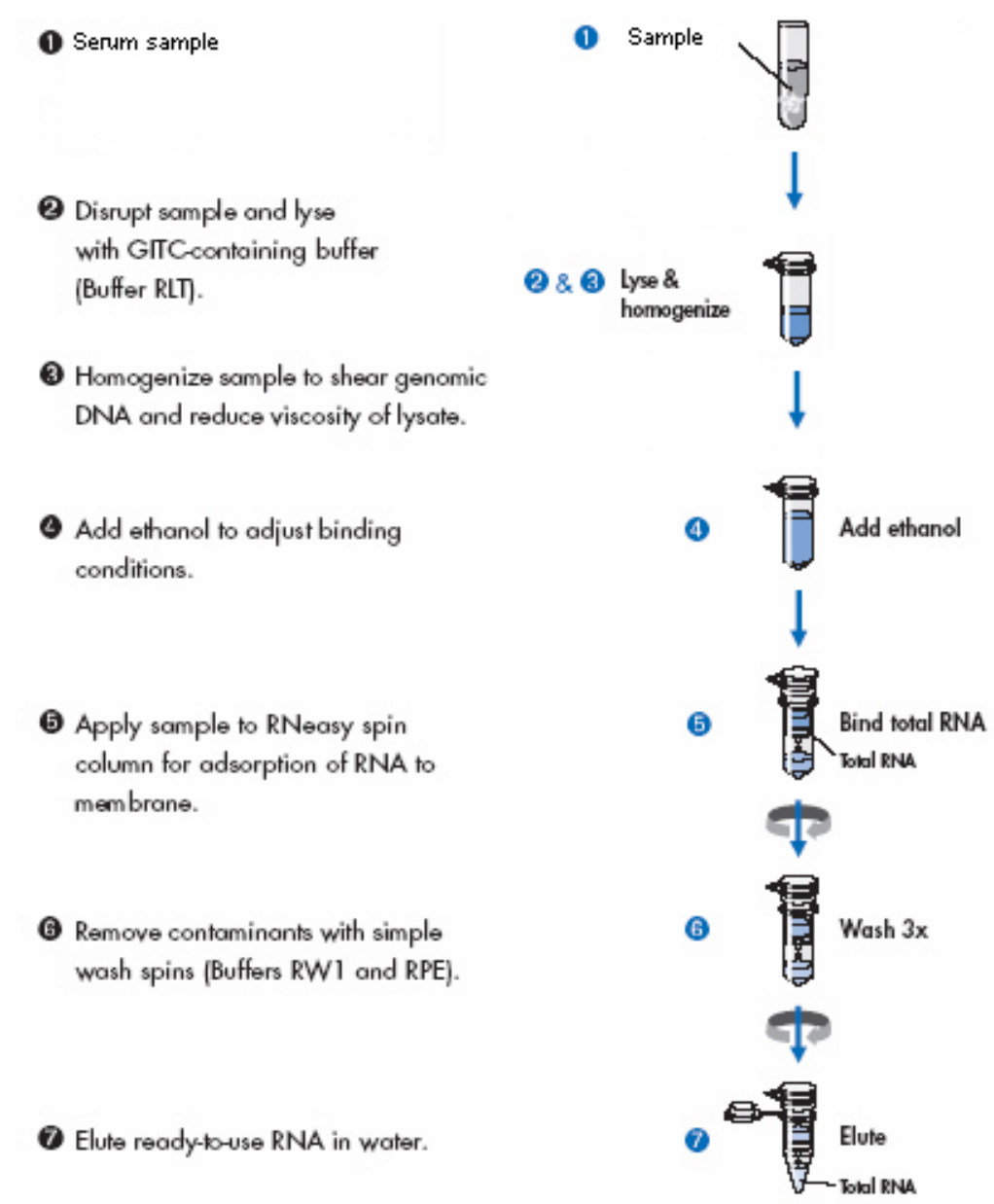

Figure 8 RNeasy Total RNA Kit flowchart.

Source: Adapted from Qiagen (2001)

Standardization of RT-nPCR

1. The First-Strand cDNA Synthesis Using Random or Oligo(dT) Primers

Genomic RNA of FIP2, FIP2B and FIP3 sample and vaccine virus was extracted using the RNeasy Total RNA Kit (Qiagen, GmbH Germany) according to the manufacturer's instruction. The first-strand cDNA was synthesized by using either random primer or oligo$(dT)_{12-18}$ primer in the reaction. The cDNA was synthesized in a 20 µl total reaction volume containing 7 µl of RNA, RT buffer 10X (KCl 37.5 mM, Tri-HCl 25.0 mM, pH 8.3), 5 mM $MgCl_2$, 10 mM of each dNTP, 0.01 M DTT, 0.5 µg random primer or 0.5 µg oligo$(dT)_{12-18}$ primer, 20U RNaseOUT Recombinant RNase Inhibitor, 50 U SuperScript™ II RT. The RNA was denatured at 70 °C for 10 minutes. The cDNA was synthesized at 42°C for 50 minutes following by incubation at 70 °C for 15 minutes. RNA template was removed from the cDNA:RNA hybrid molecule by digestion with RNase H after first-strand synthesis.

Subsequently, 20 µl of each of the RT reaction mixture was added to 80 µl of the FIPV-PCR mixture and regular nested PCR was performed. The FIPV-PCR mixture consisted of 10X PCR buffer (KCl 50.0 mM, Tris-HCl 10.0 mM, pH 8.3), 2 mM $MgCl_2$, 5 mM each dNTP, 5 pmol sense primer FIP251, 5 pmol antisense primer FIP621 and 1 U of Taq DNA polymerase (Invitrogen) and placed in a thermal cycler. The temperature cycling protocol consisted of 10 minutes of preheating at 94 °C followed by 35 cycles of 30 second of denaturation at 94 °C, 30 second of primer annealing at 53 °C and 30 second of primer extension at 72 °C. Four microliters of the first amplification reaction mixture were used for a second round of amplification with the nested pair of primers, FIPs361 and FIPs530, in a 100 µl reaction volume by using above condition and cycling procedures. A 15 µl of each sample from final PCR products were analyzed in a 1.5% agarose gel.

2. RT and Multiplex-nPCR

Genomic RNAs of PN63, PN64, PN66, PN69, PN71 and FIP12 serum samples were extracted using the RNeasy Total RNA Kit (Qiagen, GmbH Germany) according to the manufacturer's instruction. The RNA isolated in the previous step was used as a template for cDNA synthesis. The cDNA synthesis was performed using random primers and the cDNA products were used in a multiplex-nPCR. Briefly, the cDNA was synthesized in a 20 µl total reaction volume containing 7 µl of RNA, RT buffer 10X (KCl 37.5 mM, Tri-HCl 25.0 mM, pH 8.3), 5 mM $MgCl_2$, 10 mM of each dNTP, 0.01 M DTT, 0.5 µg random primer, 20U RNaseOUT Recombinant RNase Inhibitor, 50 U SuperScript™ II RT. The RNA was denatured at 70 °C for 10 minutes. The cDNA was synthesized at 42°C for 50 minutes following by incubation at 70 °C for 15 minutes. RNA template was removed from the cDNA:RNA hybrid molecule by digestion with RNase H after first-strand synthesis.

Multiplex PCR, 10 µl of the RT reaction mixture was added to 40 µl of the multiplex PCR mixture. The multiplex PCR mixture consisted of 10X PCR buffer (KCl 50.0 mM, Tris-HCl 10.0 mM, pH 8.3), 2 mM $MgCl_2$, 5 mM dNTP mix, 5 pmol of each outer primer (FIP205, FIP211, FIP251, FIP621) and 1 U of Taq DNA polymerase (Invitrogen) before placed in a thermal cycler. The temperature cycling protocol consisted of 10 minutes of preheating at 94 °C followed by 35 cycles of 30 seconds of denaturation at 94 °C, 30 seconds of primer annealing at 53 °C and 30 seconds of primer extension at 72 °C. Four microliters of the first amplification reaction mixture were used for a second round of each amplification with the nested pair of primers. The internal pair of primers for FCoV PCR were FIPg276 and FIPg204 and for FIPV PCR were FIPs361 and FIPs530. The nested PCR was performed in a 100 µl reaction volume by using the condition and cycling mentioned previously. A 15 µl of each sample from final multiplex-nPCR products were analyzed in a 1.5% agarose gel. A hundred bp DNA leader was used as a molecular weight marker.

3. RT-nPCR Procedure

3.1 First-strand cDNA synthesis The RNA isolated in the previous step was used as a template for cDNA synthesis. The cDNA was synthesized in a 20 µl total reaction volume containing 7 µl of RNA, 10X RT buffer (KCl 37.5 mM, Tri-HCl 25.0 mM, pH 8.3), 5 mM $MgCl_2$, 10 mM of each dNTP, 0.01 M DTT, 0.5 µg random primer, 20U RNaseOUT Recombinant RNase Inhibitor, 50 U SuperScript™ II RT. The RNA was denatured at 70 °C for 10 minutes. The cDNA was synthesized at 42°C for 50 minutes following by incubation at 70 °C for 15 minutes. The random hexamer was used for cDNA systhesis because the target sequence for amplification (S1 region) is far from the poly(A). RNA template was removed from the cDNA:RNA hybrid molecule by digestion with RNase H after first-strand synthesis.

3.2 nPCR amplification To perform FCoV PCR, 20 µl of the RT reaction mixture was added to 80 µl of the PCR mixture. The PCR mixture consisted of 10X PCR buffer (KCl 50.0 mM, Tris-HCl 10.0 mM, pH 8.3), 2 mM $MgCl_2$, 5 mM each dNTP, 5 pmol sense primer FIP205, 5 pmol antisense primer FIP211 and 1 U of Taq DNA polymerase (Invitrogen) and placed in a thermal cycler. The temperature cycling protocol consisted of 10 minutes of preheating at 94 °C followed by 35 cycles of 30 seconds of denaturation at 94 °C, 30 seconds of primer annealing at 53 °C and 30 seconds of primer extension at 72 °C. Four microliters of the first amplification reaction mixture were used for a second round of amplification with the nested pair of primers, FIPg276 and FIPg204, in a 100 µL reaction volume by using the same condition and cycling procedure.

For FIPV PCR, 20 µl of the RT reaction mixture was added to 80 µl of the PCR mixture that consisted of 10X PCR buffer (KCl 50.0 mM, Tris-HCl 10.0 mM, pH 8.3), 2 mM $MgCl_2$, 5 mM each dNTP, 10 pmol sense primer FIP251, 10 pmol antisense primer FIP621 and 1 U of *Taq* DNA polymerase. The reaction tube was then placed in a thermal cycler. The temperature cycling for the FIPV PCR was similar to that of FCoV PCR. Four microliters of these amplification products were then subjected to a second round of

amplification by using the same cycling procedure after adding the internal or nested primers, FIPs361 and FIPs530, in a 100 µl reaction volume by using the same condition and cycling procedure.

Analysis of PCR-Amplified Products

A 15 µl of each sample from final PCR products were analyzed in a 1.5% agarose gel, 100 bp DNA Leader was used as a molecular weight marker. Amplification products were visualized by ethidium bromide staining and UV light transillumination. Samples revealing a band of 177 bp after the nested PCR were considered positive for FCoV RNA. For FIPV, the amplification products after the second, nested amplification were appeared as a band of 170 bp when the target sequence was present in the sample. No band was evident when the target sequence was not present in the sample.

Detection of Antibodies to FCoV

1. Enzyme-Linked Immunosorbent Assay (ELISA)

Antibodies against FCoV were detected by ELISA, using ImmunoComb® FCoV Antibody Test Kit (Biogal Galed Laboratories, Israel). The ImmunoComb® test is a modified ELISA that detects IgG antibody levels in serum or whole blood. The ImmunoComb® FCoV Antibody Test Kit composes of a comb-shaped plastic card (Comb) and a multi-compartment developing plate. The Comb contains 3 spots. In the test spot, FCoV antigens were attached to the lowest spot on the Comb. The middle spot is the positive reference and the upper most spot is the internal control (Figure 9).

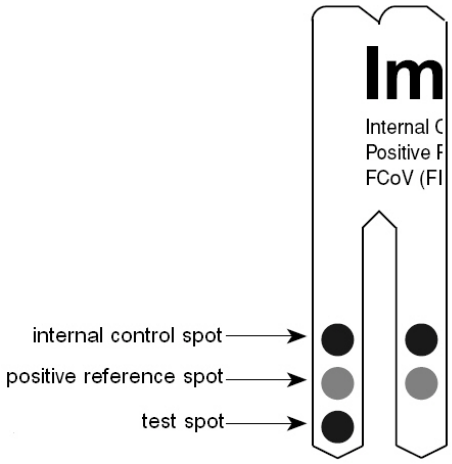

Figure 9 **Example of two teeth of a developed comb.**

Source: Adapted from Biogal Galed Laboratories (2004)

First, each serum sample was added in each well in row A of the multi-compartment developing plate. Next, the Comb was transferred to the remaining wells (B-F). In the row B, non-bound antibodies were washed off. Row C contained an enzyme labeled anti-cat IgG antibody, which would bind to the antigen-antibody complexes at the test spots. The Comb was washed for additional two times in rows D and E. Then, the Comb was moved to the next well (row F), where a color was developed by an enzymatic reaction (Figure 10).

2. Reading and Interpreting ELISA Results

The Comb contains 3 spot (Figure 9). The upper spot (internal control spot) gave a dark grey color to demonstrate that all components functioned well. The middle spot (positive reference spot) containing positive antibodies presented a distinct grey color that was generated by a significant positive IgG response. This spot was always read as S3 on the CombScale (a scale of S0 to S6) (Figure 11). The bottom spot on the Comb was test the spot for FCoV antibodies. To read the result, the level of positive color of the bottom spot was compared to the positive reference spot. A visible grey dot indicated a positive response to FCoV. The color darker than that of the positive reference

represented high FCoV antibody titer, while the fainter color than that of the positive reference showed low FCoV antibody response. A negative result (less than S1) indicated that the cat had not been exposed or had cleared the virus. Thus, it was free of FCoV.

Perform assay at room temperature of 20°-25°C

1. Obtain serum sample from cat.

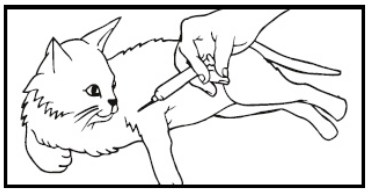

2. Deposit a 5 µl serum sample into well in row A of Developing plate and incubate for 60 minutes.

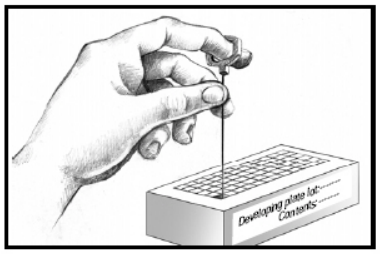

3. Insert the Comb into the wells in row A and incubate for 10 minutes.

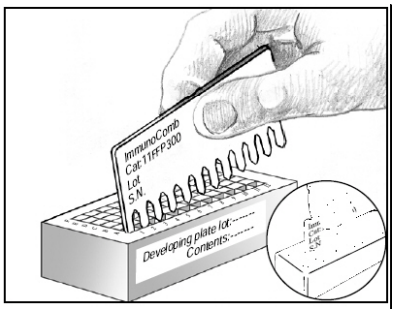

4. Insert the Comb into the wells in row B for 2 minutes. Then, place Comb in remaining wells (row C for 10 min., row D&E for 2 min., and row F for 10 min.).

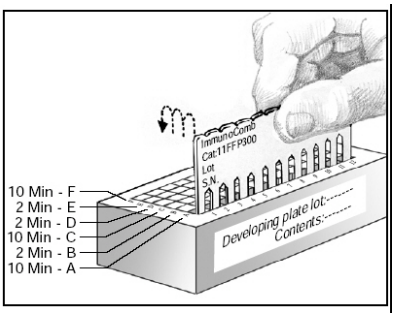

5. Upon completion of the color development in row F, move the Comb back to row E for 2 minutes to fix color. Take the Comb out and air dry.

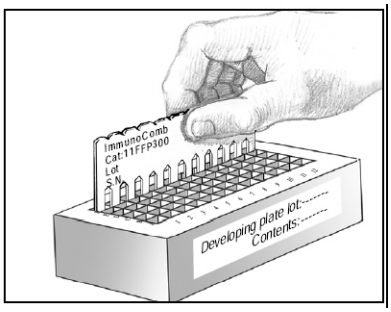

Figure 10 **ImmunoComb® FCoV Antibody Test Kit flowchart.**

Source: Adapted from Biogal Galed Laboratories (2004)

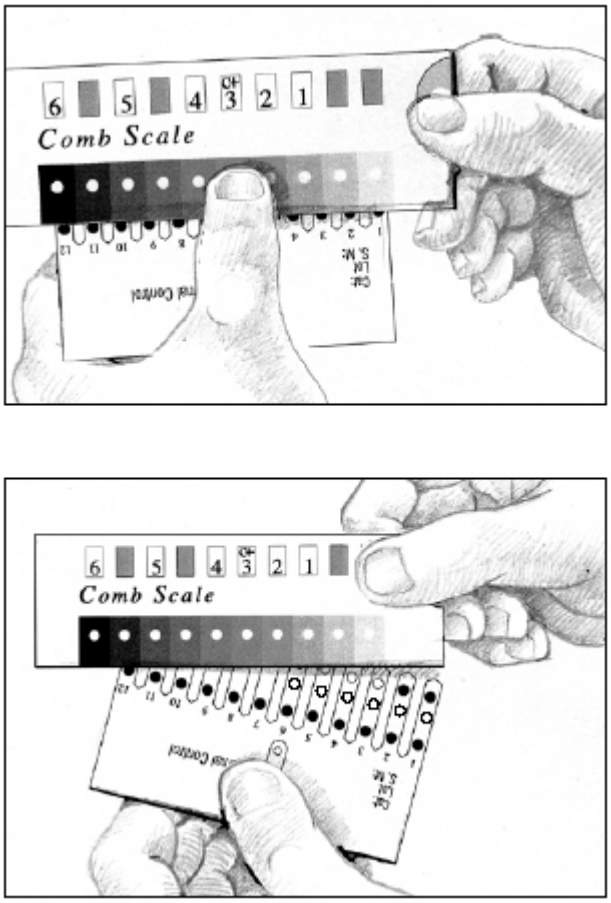

Figure 11 The Comb Scale

Source: Biogal Galed Laboratories (2004)

RESULTS

Samples

A total of 190 serum samples (PN2-177 and T1-14) were randomly collected from cats in the central and eastern part of Thailand. The serum samples were from cats at the age range from one month to 18 years. Majority of the samples were from collected from various breeds including short hair native (164), 1 Kawmanee (1), 1 Korat (1), 2 Vichenmas (2) and Persian (10) cats. The proportions of cats classified by sex were 54.4% females and 45.5% male. Three samples were effusive fluids from sick cats visiting Small Animal Teaching Hospital of Kasetsart University. Two of the samples (FIP3 and FIP12) were cats falling in FIP case definition, while one cat (FIP2) did not match the clinical criteria. RNA was isolated from 184 out of 190 samples while 104 samples were examined for the presence of antibodies to FCoV. Not all samples were tested for both assays because there was limited amount of some samples.

Efficiency of Different RT-nPCRs

1. Random Versus Oligo(dT) Primers in cDNA Synthesis

The results showed that either random or oligo(dT) primer could be applied in the FIPV RT-nPCR. Both primers were able to initiate the transcription of RNAs from vaccine virus and FIP3. The resulting cDNAs were used in FIPV-nPCR and yielded a FIPV specific DNA of 170 bp. However, RT-nPCR performed using oligo(dT) in RT reaction and FIPV specific primers in nPCR yielded negative result (Figure 12a; lane 4) with RNA isolated from FIP2. When the similar cDNA reaction was used in FCoV-nPCR, it gave rise a 177 bp DNA fragment specific to FCoV. On the other hand, the reverse transcription primed by random primers was proceeded using FIP2 RNA as the template prior to performed nPCR for FIPV, the DNA fragment of 170 bp specific for FIPV appeared clearly. This indicates that there was FIPV RNA in the FIP2 RT-nPCR reaction

but oligo(dT) failed to prime cDNA synthesis of S1 region from the limited amount FIPV RNA in the original sample.

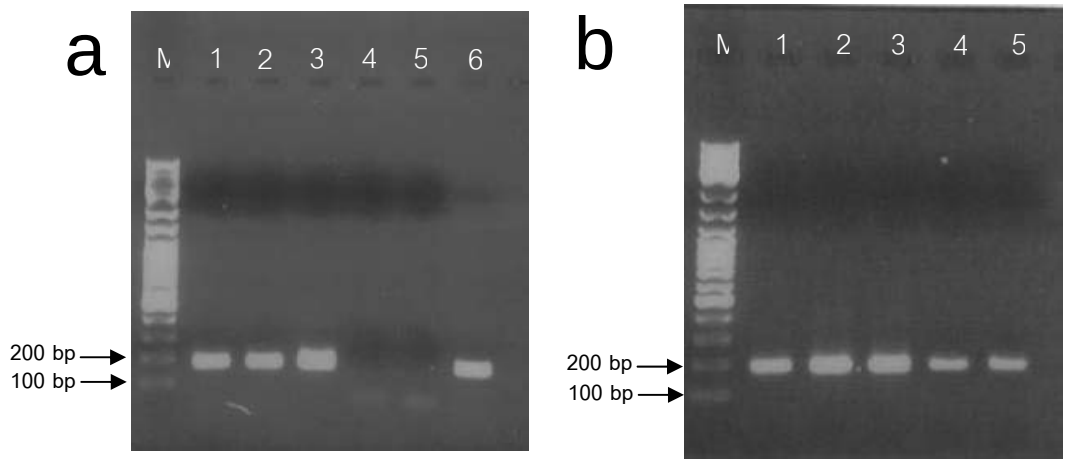

Figure 12 Electrophoretic analysis of PCR products from cDNA synthesis with either oligo(dT) (a) or random primers (b), M represents 1 kb plus DNA ladder.

a. PCR products using cDNA templates acquired from RT reaction primed by the oligo(dT) primer. Lane 1, 2 and 3: FCoV nPCR using RNA isolated from FIP2, FIP2B and FIP3, respectively, as the templates for amplification; lane 4, 5 and 6: FIPV nPCR using FIP2, FIP2B and FIP3, respectively, in the RT-PCR process.

b. PCR products which are amplified from cDNA synthesized using random primer. Lane 1: FIPV-nPCR amplified from FIP2 template; lane 2 and 3: FCoV-nPCR using vaccine virus and FIP3 RNA as the templates for amplification; lane 4 and 5: FIPV RT-nPCR amplified from vaccine virus and FIP3 RNA.

2. Muliplex-nPCR Versus nPCR

cDNA synthesis using random primers were performed from total RNA isolated from serum samples (PN63, PN64, PN66, PN69 and PN71) and the effusive fluid from a FIPV cat (FIP12). The cDNA products were then further amplified using two nested PCR. The first PCR was multiplex-nPCR in which the cDNAs were amplified using 2 pairs of outer primers; one was specific for FCoV and another targeted FIPV. This was followed by 2nd round of nested PCR using 2 pairs of internal primers specific for FCoV and FIPV, respectively. The second method was the regular nPCR in which the cDNAs were transferred into two separated tubes containing outer primers specific for either FCoV or FIPV. The first PCR products were used for 2nd round nPCR using specific internal primers specific for FCoV or FIPV in separated tubes.

The results showed that the multiplex-nPCR was able to amplified 4 out of 6 of tested samples as the appearance of 177 bp specific for FCoV (Table 5). With equal amount and conditions of cDNA, all tested samples were FCoV positive by the regular nPCR. Thus, it is indicated that the regular nPCR might be more sensitive than multiplex-nPCR for the detection of FCoV. However, both assays were able to amplified FIPV specific cDNA from a sample (FIP12) as shown in table 5. In addition, we did not attempt to intensively compare the sensitivity of both assays for the detection of FIPV since there were very few FIPV positive samples with limited amount in our laboratory.

Table 5 Comparison results of multiplex nPCR with regular nPCR techniques

Sample number	Multiplex nPCR		Regular nPCR	
	FCoV nPCR	FIPV nPCR	FCoV nPCR	FIPV nPCR
PN63	+	-	+	-
PN64	-	-	+	-
PN66	+	-	+	-
PN69	+	-	+	-
PN71	-	-	+	-
FIP12	+	+	+	+

Note: -, negative; +, positive

Prevalence of FCoV and FIPV

1. Proportion of Cats Harboring FCoV and/or FIPV RNA

The sera and effusive fluids collected from cats in the central and eastern part of Thailand were examined for the presence of FCoV and FIPV RNAs. Total RNAs were isolated from 184 serum samples (PN2-18, PN20-38, PN40-57, PN60-61, PN63-79, PN83-177, T1-10 and T12-14) and 3 effusive fluids (FIP2-3 and FIP12) as shown in table 6. These RNAs were used as templates for cDNA synthesis using random primer. The cDNAs were amplified using outer and internal primers specific for FCoV or FIPV RNA in separated reactions of regular RT-nPCR. The feline coronavirus specific PCR product of 177 basepair was present after the nested PCR in 57 (30.97%) serum samples. The FIPV specific nPCR product is 170 basepair. FIPV RNA was also detected in three (1.63%) serum samples (Table 6 and 7). Figure 13 and 14 demonstrate RT-nPCR products of serum samples containing FCoV and FIPV RNA, respectively.

Table 6 Results of serum samples and effusive fluids examined for the presence of FCoV or FIPV RNA, antibodies to FCoV as well as clinical signs resemble FIP.

Sample No.	Immunocomb	FCoV RT-nPCR	FIPV RT-nPCR	Signs
PN2	+	+	-	-
PN3	INVALID[a]	-	-	-
PN4	+	-	-	-
PN5	INVALID[a]	+	-	INVALID[b]
PN6	M	+	-	M
PN7	+	+	-	-
PN8	INVALID[a]	+	-	-
PN9	+	-	-	+
PN10	+	+	-	-
PN11	+	-	-	-
PN12	+	-	-	-
PN13	+	-	-	-
PN14	+	-	-	-
PN15	+	-	-	+
PN16	-	+	-	-
PN17	+	-	-	+
PN18	+	-	-	-
PN19	+	M	M	-
PN20	+	-	-	-
PN21	+	-	-	+
PN22	-	-	-	-
PN23	+	-	-	-
PN24	-	-	-	+

Table 6 (Continued)

Sample No.	Immunocomb	FCoV RT-nPCR	FIPV RT-nPCR	Sign
PN25	+	-	-	-
PN26	M	-	-	M
PN27	M	+	-	M
PN28	M	+	-	M
PN29	M	-	-	M
PN30	M	-	-	M
PN31	M	-	-	M
PN32	M	-	-	M
PN33	M	-	-	M
PN34	M	-	-	M
PN35	M	-	-	M
PN36	M	-	-	M
PN37	M	-	-	M
PN38	M	-	-	M
PN40	M	-	-	M
PN41	M	-	-	M
PN42	M	-	-	M
PN43	M	-	-	M
PN44	M	-	-	M
PN45	M	-	-	M
PN46	M	-	-	M
PN47	M	-	-	M
PN48	M	-	-	M
PN49	M	-	-	M
PN50	M	-	-	M

Table 6 (Continued)

Sample No.	Immunocomb	FCoV RT-nPCR	FIPV RT-nPCR	Sign
PN51	+	-	-	+
PN52	-	-	-	-
PN53	+	-	-	-
PN54	+	-	-	+
PN55	+	+	-	-
PN56	+	+	-	-
PN57	+	+	-	-
PN58	+	M	M	-
PN59	+	M	M	-
PN60	M	+	-	M
PN61	-	-	-	-
PN63	-	+	-	-
PN64	-	+	-	-
PN65	+	-	-	-
PN66	-	+	-	-
PN67	-	+	-	-
PN68	-	+	-	-
PN69	-	+	-	-
PN70	-	-	-	-
PN71	-	+	-	-
PN72	+	-	-	-
PN73	-	+	-	-
PN74	-	-	-	-
PN75	+	-	-	-
PN76	+	-	-	-

Table 6 (Continued)

Sample No.	Immunocomb	FCoV RT-nPCR	FIPV RT-nPCR	Sign
PN77	-	-	-	-
PN78	-	+	-	-
PN79	-	-	-	-
PN80	-	M	M	M
PN81	+	M	M	M
PN82	+	M	M	M
PN83	-	-	-	-
PN84	-	-	-	-
PN85	INVALID[a]	+	-	-
PN86	INVALID[a]	-	-	-
PN87	+	-	-	-
PN88	+	-	-	-
PN89	+	+	-	-
PN90	M	+	+	+
PN91	+	+	-	-
PN92	+	+	-	+
PN93	+	+	-	-
PN94	-	+	-	-
PN95	-	+	-	-
PN96	-	+	-	-
PN97	M	+	-	M
PN98	+	+	-	-
PN99	-	+	-	-
PN100	M	+	-	M
PN101	M	+	-	M

Table 6 (Continued)

Sample No.	Immunocomb	FCoV RT-nPCR	FIPV RT-nPCR	Sign
PN102	M	+	-	M
PN103	M	+	-	M
PN104	M	+	-	M
PN105	M	+	-	M
PN106	M	+	-	M
PN107	-	-	-	M
PN108	-	-	-	M
PN109	+	-	-	M
PN110	+	-	-	M
PN111	-	-	-	M
PN112	+	-	-	M
PN113	INVALID[a]	-	-	M
PN114	+	-	-	M
PN115	+	-	-	M
PN116	-	-	-	M
PN117	-	-	-	M
PN118	-	-	-	M
PN119	+	-	-	M
PN120	+	+	-	M
PN121	+	-	-	M
PN122	+	+	-	M
PN123	-	-	-	M
PN124	+	-	-	M
PN125	-	-	-	M
PN126	-	-	-	M

Table 6 (Continued)

Sample No.	Immunocomb	FCoV RT-nPCR	FIPV RT-nPCR	Sign
PN127	-	-	-	M
PN128	-	-	-	M
PN129	-	-	-	M
PN130	-	-	-	M
PN131	-	-	-	M
PN132	-	+	-	M
PN133	+	-	-	M
PN134	-	-	-	M
PN135	+	-	-	M
PN136	+	-	-	M
PN137	+	-	-	M
PN138	+	-	-	M
PN139	+	+	-	M
PN140	-	-	-	M
PN141	-	-	-	M
PN142	+	-	-	M
PN143	M	-	-	M
PN144	M	-	-	M
PN145	M	+	-	M
PN146	M	-	-	M
PN147	M	+	-	M
PN148	M	-	-	M
PN149	M	-	-	M
PN150	M	-	-	M
PN151	M	+	-	M

Table 6 (Continued)

Sample No.	Immunocomb	FCoV RT-nPCR	FIPV RT-nPCR	Sign
PN152	M	-	-	M
PN153	M	-	-	M
PN154	M	-	-	M
PN155	M	-	-	M
PN156	M	-	-	M
PN157	M	-	-	M
PN158	M	+	-	M
PN159	M	-	-	M
PN160	M	-	-	M
PN161	M	+	-	M
PN162	M	-	-	M
PN163	M	-	-	M
PN164	M	-	-	M
PN165	M	-	-	M
PN166	M	-	-	M
PN167	M	+	-	M
PN168	M	-	-	M
PN169	M	-	-	M
PN170	M	-	-	M
PN171	M	-	-	M
PN172	M	-	-	M
PN173	M	-	-	M
PN174	M	-	-	M
PN175	M	-	-	M
PN176	M	+	-	M

Table 6 (Continued)

Sample No.	Immunocomb	FCoV RT-nPCR	FIPV RT-nPCR	Sign
PN177	M	-	-	M
T1	M	-	-	M
T2	M	-	-	M
T3	M	-	-	M
T4	M	+	-	M
T5	M	-	-	M
T6	M	+	-	M
T7	M	-	-	M
T8	M	+	-	M
T9	M	-	-	M
T10	M	-	-	M
T12	M	-	-	M
T13	M	-	-	M
T14	M	-	-	M
FIP2	M	+	-	-
FIP3	M	+	+	+
FIP12	M	+	+	+

Note: M, missing data; -, negative; +, positive; INVALID[a], internal control invalid and no serum left for additional assay; INVALID[b], no information of clinical signs

Table 7 Proportion of cats from the central and eastern part of Thailand which were positive for FCoV and FIPV RNAs tested by RT-nPCR or antibodies to FCoV examined by dot blot ELISA.

Number of samples / Assays	Positive (%)	Negative	Total
FIPV nPCR	3 (1.63%)	181	184
FCoV nPCR	57 (30.97%)	127	184
ELISA	55 (56.12%)	43	98

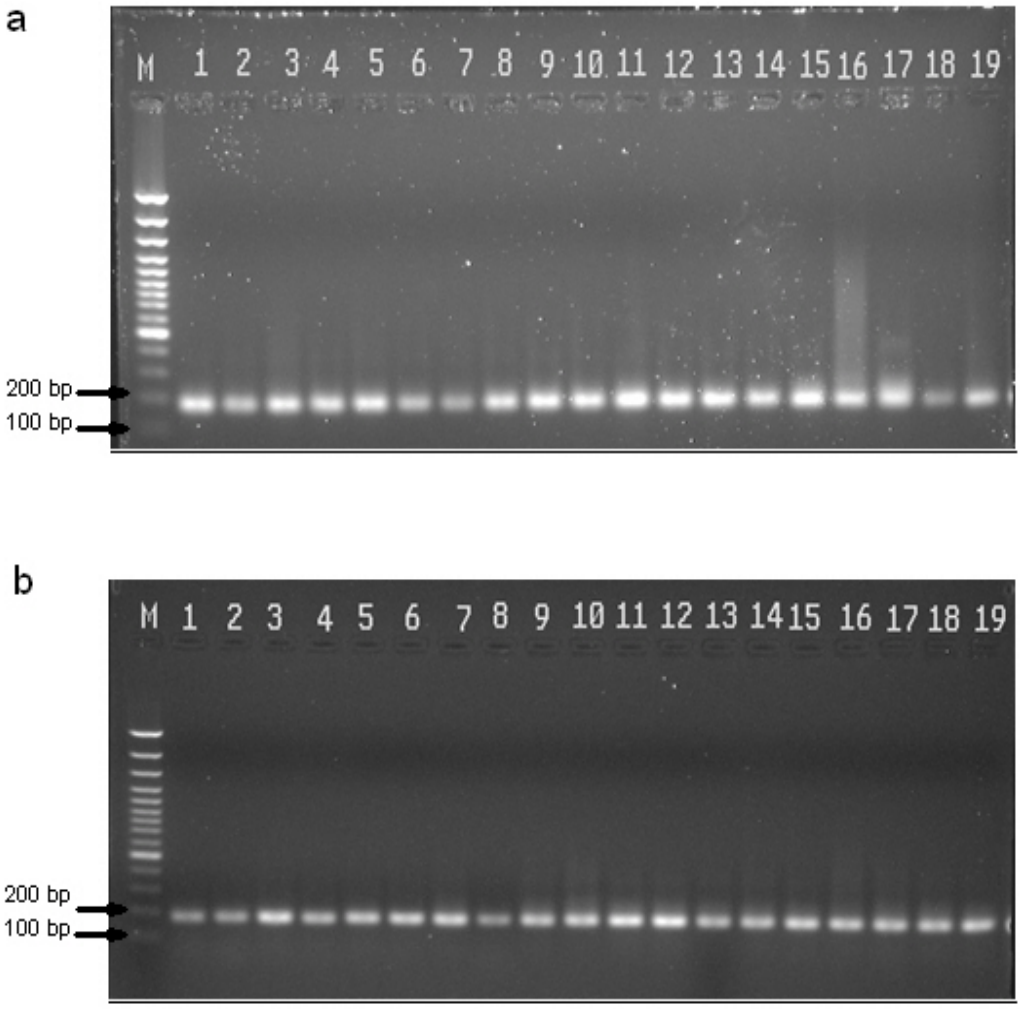

Figure 13 Electrophoretic analysis of PCR products from FCoV RT-nPCR positive samples, M represents 100 bp DNA ladder.

a. Lane 1, FIP vaccine strain; lanes 2-19, serum samples positive for FCoV nPCR: FIP2, FIP3, FIP12, PN2, PN5, PN6, PN7, PN8, PN10, PN16, PN27, PN28, PN55, PN56, PN57, PN60, PN63 and PN64, respectively.

b. Lanes 1-19, serum sample positive for FCoV nPCR: PN66, PN67, PN68, PN69, PN71, PN73, PN78, PN85, PN89, PN90, PN91, PN92, PN93, PN94, PN95, PN96, PN97 and PN98, respectively.

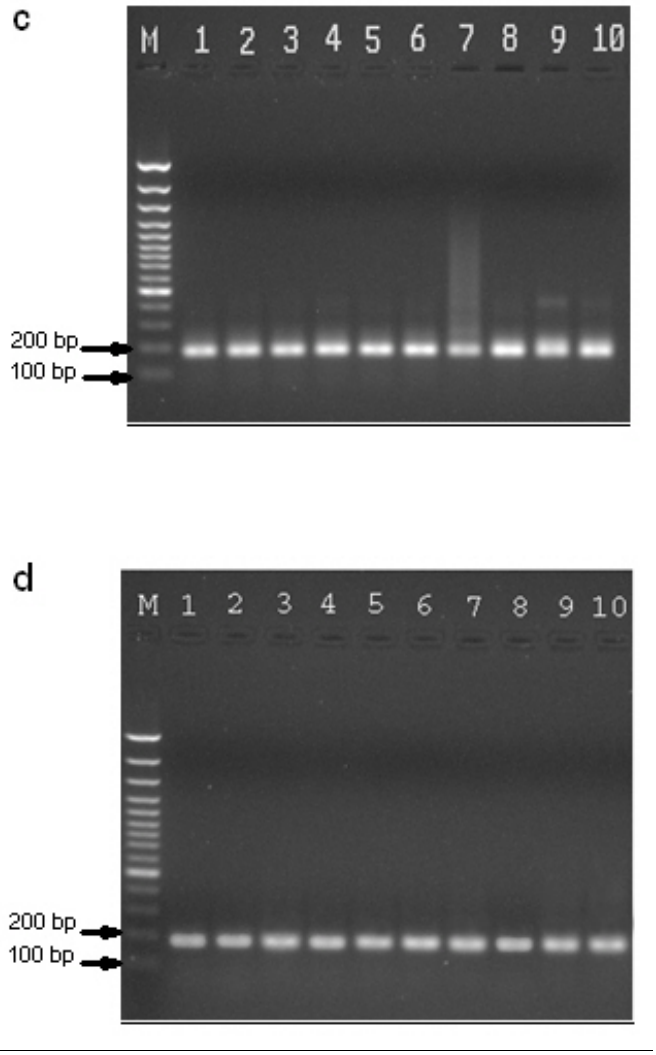

Figure 13 (Continued)

c. Lanes 1-10, serum sample positive for FCoV nPCR: PN100, PN101, PN102, PN103, PN104, PN105, PN106, T4, T6 and T8, respectively.

d. Lanes 1-10, serum sample positive for FCoV nPCR: PN120, PN122, PN132, PN139, PN145, PN147, PN151, PN158, PN167 and PN176, respectively

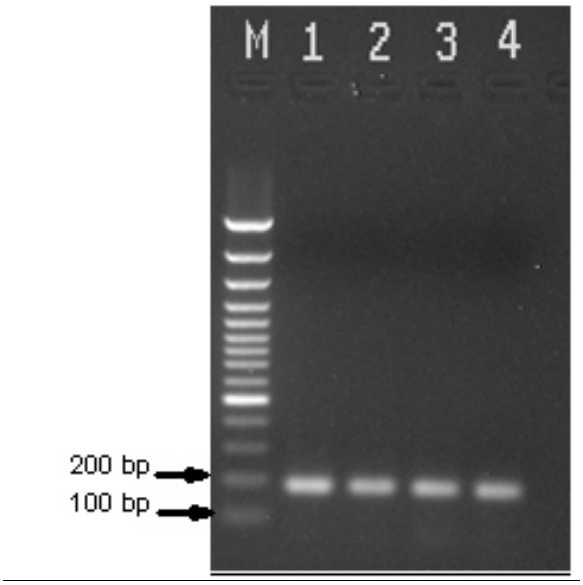

Figure 14 Electrophoretic analysis of PCR products from FIPV RT-nPCR positive samples, M represents 100 bp DNA ladder. Lanes 1, FIP vaccine strain; lanes 2-4, serum sample positive for FIPV nPCR, FIP3, FIP12 and PN90, respectively.

2. Proportion of Cats with FCoV Antibodies

In addition to examination for the viral RNA, the 104 serum samples were tested for the presence of FCoV antibodies in a dot blot ELISA technique using Immunocomb FCoV Antibody Test Kit (Biogal Galed Laboratories, Israel). Six out of 104 samples were invalid since the dark blue color did not develop in the internal control slot. Therefore 98 samples were interpreted for the presence of FCoV antibodies. The results were demonstrated in table 6 and 7. Antibodies to FCoV were detected in sera of 55 from 98 cats (56.12%).

The results of serum samples examined by both RT-nPCR and dot blot ELISA were compared (Table 8). Out of 92 samples, 14 sera contained both FCoV RNAs and antibodies against FCoV. Twenty-seven cats were negative for both FCoV and its antibodies, indicating that these cats had never exposed to FCoV. Sera of 36 out of 92 cats contained antibodies to FCoV but no FCoV RNA was detected. This suggested that the cats might be previously infected with FCoV. FCoV RNAs were detected in sera of 15 cats without the presence of antibodies to FCoV. It is possible that these cats are infected with FCoV and are viremia.

Table 8 **Relationship between detection of FCoV RNA by RT-nPCR and detection of antibody of FCoV by ImmunoComb**

FCoV-nPCR / Immuno comb	Negative	Positive	Total
Negative	27	15	42
Positive	36	14	50
Total	63	29	92

CONCLUSION AND DISCUSSIONS

Feline infectious peritonitis, a fatal, immune-mediated disease of domestic and wild cats is caused by FIPV, a mutant of FCoV. FIPV infection in cats were reported in European countries (Pedersen, 1995; Holst *et al*., 2005; Cave *et al*., 2004), Australia (Bell et al., 2006), United State of America (Kennedy *et al*., 2002) and Japan (Hohdatsu *et al*., 1992). Serological studies of FCoV in European countries showed that 25% of household cats and up to 80 to 90% in multicat household and catteries had FCoVs antibodies (Pedersen, 1995). The prevalence of antibodies against FCoV was 31% in Swedish cats (Holst *et al*., 2005) and 25.6% in British cats (Cave *et al*., 2004). Serological survey of antibodies to FCoV in Sydney cats in Australia resulted in 34% seropositive (Bell *et al*., 2006).

This present study is the first report of the appearance of FCoV and FIPV infection in cats in Thailand. We revealed that out of 184 serum samples collected from cats in the central and eastern parts of Thailand 30.97% was positive for FCoV and 1.63% was positive for FIPV when examined by RT-nPCR. The prevalence of FCoV found (30.97%) by RT-nPCR was in accordance with the aforementioned studies that used serological methods to detect antibodies to FCoV. In this present study, the serological survey using a dot blot assay (ImmunoComb® FCoV Antibody Test Kit) to detect the presence of antibodies to FCoV in the serum samples demonstrates 56.12% seropositive cats. This number is slightly high prevalence for household cats.

The previous studies revealed that number of cats with anti-FCoV antibodies are higher in purebred cats than in mixed breed cats and in the multicat household than in the household cats (Cave *et al*., 2004; Holst *et al*., 2005; Bell *et al*., 2006). However, number of FCoV seropositive cats was found equally between male and female cats. In one of the studies, the serum samples were randomly collected from cats with different breeds, management (household and multicat household), sex, health and age (a month

to eighteen years) (Pesteanu-Somogyl *et al*., 2006). The results suggested that the purebred young cats at 3 months to three years of age were at high risk to develop FIP.

In a study in USA, the prevalence of FCoV surveyed from seventy-five samples using serological method (immunofluorescence) found that 29 (38.66%) were seropositive to type I and/or type II FCoV. The prevalence of FCoV detected by RT-PCR were 24 (32.0%) which 13 (17.33%) samples were seronegative to FCoV type I and type II but positive using RT-nPCR for FCoV. In addition, 20 (26.66%) were seropositive but gave rise negative result using RT-PCR for FCoV. The results showed that serological method may be not correlative with virus shedding (Kennedy *et al*., 2002). In a parallel study, the prevalence of FCoVs detected by serological method was higher than the rate observed by RT-nPCR. Fifteen samples (16.30%) were seronegative to ImmunoComb but were positive for FCoV RNA using RT-nPCR. On the other hand, 36 (39.13%) were seropositive but yielded negative result using RT-nPCR for the detection of FCoV. This suggests the presence of coronavirus antibodies in non-viremic cats. Cats with serological positive represent the cats previously exposed to the coronavirus, which may not necessarily shed or carry FCoVs. The RT-nPCR used in this study detected the presence of FCoV and FIPV in serum samples. However, this technique can not detect FCoV RNA in all of the cats with FIP since 6.4% of the samples of cat with FIP were negative when detected by FCoV RT-nPCR as described by Herrwegh et al. (1995) (Benetka et al., 2004). In accordantly, our study showed that the FCoV infection rate as detected by serological method was higher than as detected by RT-nPCR. The higher prevalence observed by serological method compared with that determined by RT-nPCR suggests the presence of coronavirus antibodies in non-viremic cats (Kennedy *et al*., 2002). Cats with serological positive represent the cats previously exposed to the coronavirus, which may not necessarily shed or carry FCoV. The RT-nPCR used in this study detected the presence of FCoV and FIPV nucleic acid in the serum samples. Only does viremic cats that contain FCoV in blood will give raise the positive results. This

would explain the discrepancy results between FCoV seropositive cats (56.12%) and cats with FCoV RNA (30.97%).

Usually 10-20% of RNA extracted by using the binding of RNA to the membrane in a column may be lost (RNeasy Total RNA Kit (QIAGEN®) handbook). This may cause false negative detection in case that the viral RNAs in the serum samples are low. However, in the RNA isolation process poly C carrier RNA was applied to the extracted RNA solution to increase the RNA yield. Addition of poly C carrier may slightly enhance the sensitivity of our FCoV and FIPV RT-nPCR.

When two methods of FIPV RT-nPCR were compared, the results showed that the random primer primed RT-nPCR seems to be slightly more sensitive than oligo(dT) primed reverse transcription. The differences in the DNA yields may in part come from the distances between the primers and the amplified targets. The target sequence for FIPV specific primers lies within S1 region, which is far away from the poly (A) tail, the position hybridized by the oligo(dT). Thus, the amount and complexity of cDNA may decrease process of the reverse transcriptase. The most non-specific primer, random primers, is able to utilize all RNA population as templates for first-stand cDNA synthesis and may maximize the size of cDNA. However, for FCoV RT-nPCR, whether using the oligo(dT) or random primer in cDNA synthesis may be almost similar because the target position, 3'-UTR, is near the poly (A) tail, the primer annealing region. In addition to use random or oligo(dT) in cDNA synthesis, a gene-specific primer that hybridized close to the S gene of FCoV may directly increase the template for amplification, resulting in more sensitivity.

We also found that multiplex RT-nPCR is less sensitive than regular RT-nPCR. In case that the amount of the viruses in the samples are low, multiplex RT-nPCR should not apply for the detection of FIPV since it may cause false negative. However, if the

samples are collected from FIP cats, this multiplex RT-nPCR may be used to save time and reagents.

The results of this present study suggest that FCoV RT-nPCR seems to be more sensitive than FIPV RT-nPCR. All samples positive for FIPV RNA are also positive for FCoV while some of FCoV positive sera were FIPV negative. A previous study also demonstrated that 10% of FCoV infected cats developed FIP (Vennema et al., 1998) indicating that FCoV in some cats may not mutate to FIPV. The prevalence of FIP in the purebred cats included in this study such as Siamese and Persian were found to be as low as 0.2% for Siamese and 0.5% for Persian (Pesteanu-Somogyl *et al*., 2006). Most of samples in this study were from mix bred cats which developed FIP at low rate too.

The very low rate of FIPV, 1.63%, as detected by RT-nPCR may be also due to false negative because high variability in the S1 region (Gamble *et al*., 1997; Benetka *et al*., 2004). The target sequence chosen for our FIPV RT-nPCR may not detect all strains of FIPV, including FIPV in Thailand. The pair of primers was tested in three FIPV strains including UCD-1, NOR-15 and the modified live, temperature-sensitive mutant FIP vaccine strain. The UCD-1 is representing FIPV derived from FCoV type I and NOR-15 is FCoV type II. So, the primers may not match with other FIPV strains and isolates. The secondary structure in S region of the viral RNA template may cause false negative because low temperature (42^{O}C) was used in cDNA synthesis. Although random primer was utilized to avoid the secondary structure problem, the higher RT incubation temperature, eg. 70^{O}C, may be able to help disrupt RNA secondary structure and increase the yield of cDNA (ThermoScript™ Reverse Transcriptase (Invitrogen™) Manual).

FIPV serotypes I strain are predominant in Europe whereas type II strains have hardly been found (Rottier, 1999). In Japan and USA, FCoV type I seem to be higher prevalent (Hohdatsu *et al*., 1992; Kennedy *et al*., 2002). Although it is a very rare event,

new strain of FIPV may be occur in Thailand which cause less prevalence of FIPV in this study (if the primer using in FIPV RT-nPCR is not match). Serotype II strains are the result of double recombination between FECV type I strains and CCoV. The recombination occurs somewhere in the E and the M gene and second recombination in *pol* gene. Thus CCoV sera can neutralize FIPV type II strains but weakly neutralize type I strain (Herrewegh *et al*., 1998; Horzinek *et al*., 1995). In addition, fAPN, the receptor for type II, can bind CCoV (Tresnan et al., 1996). Thus CCoV may infect the cat or it may be involved indirectly to the recombination between FCoV type I and CCoV. FIPV arise by mutation from FECV that FIP-defining mutation may occur in the S, 3c, 7a and/or 7b gene (Foley and Leutenegger, 2001). Deletion unique to FIPV were found in 3c and/or 7b ORFs (Vennema et al., 1998) and in the 7a ORF of FCoV (Kennedy et al., 1998). It was speculate that the deletions of 7a ORF may be occur from secondary structure that "loop out" this region resulting in the viral RNA polymerase "skipping" a certain region during transcription (Kennedy et al., 1998). So, S1 region that sequences are variable (deletion and substitutions in different virus isolates) (Lai and Holmes, 2001) may arise new strain of FIPV.

Thus far, there is no individual test or criteria that can distinguish FIPV form other feline coronavirus (Addie et al., 2004). Seropositive only indicates that the cats have been infected with FCoV: prior to taking the serological test (Kennedy *et al*., 2002). Thus, ImmunoComb cannot differentiate between infection with FECV and FIPV, or cats vaccinated against FIP (ImmunoComb® FCoV Antibody Test Kit (Biogal) handbook). Cats with low ImmunoComb score may be confirmed to be FIP by immunohistochemistry (IHC) assay or vise versa (Bell *et al*., 2006). Please note that IHC is the reliable definite diagnostic test. On the other hand, false negative of ImmunoComb test may result from the formation of immune complexes. Thus, there is no or low amount of free anti-FCoV antibodies in serum to react with antigens coated on the combs.

Several PCR based methods have been developed for the detection of FCoV RNA and/or FIPV RNA. This includes a real-time PCR for quantification of FCoV RNA in which the position of primers and probe were located within 7b gene (Gut *et al*., 1999). However, the sensitivity and specificity of this assay is not reported. RT-nPCR was also developed to amplify a sequence within S region to differentiate between FCoV type I and II (Benetka *et al*., 2004). This RT-nPCR showed some false negative probably due to the variability in the S gene of FCoV. In addition, mRNA-PCR was performed by mRNA isolated from peripheral blood mononuclear cells (Simons *et al*., 2005). In this assay, the target sequence for amplification was M gene which spanned the leader sequence of FCoV genome and highly conserved region of M gene. Although it has a high specificity up to 93% but 5% of the healthy cats were positively detected. The results indicate that the viral RNA found in the mononuclear cells of healthy cats may be mRNA of avirulent strains present abundantly in the blood vessels.

RT-nPCR may not be a good definitive diagnosis. FCoV RT-nPCR cannot distinguish between infection with FCoV and FIPV, although a report showed that 78% of FCoV RT-nPCR positive samples were obtained from the FIP sick cats (Herrewegh *et al*., 1995). In our study, FIPV RT-nPCR may be less sensitive when compared with FCoV RT-nPCR, due to various factors mentioned previously. One of the studies showed that the FIPV RT-nPCR possessed sensitivity and specificity as high as 91.6% and 94%, respectively, when the tested samples were from the FIP confirmed cats (Gamble *et al*., 1997). Since FIPV is present only in cats with FIP, FCoV detected in abnormal body fluids such as abdominal and thoracic fluid is assumed to be the mutant FIPV. If the differentiation of FIPV from FCoV by both RT-nPCR is restricted only samples from body fluids, FCoV RT-nPCR is likely to be a test of choice for FIPV diagnosis. Non-effusive form of FIP is difficult to diagnosis. Thus, combination of various diagnostic methods should be considered. The positive results of immunoassay and/or FCoV RT-nPCR should be confirmed with history of cats, clinical signs and other laboratory finding.

LITERATURE CITED

Addie, D.D. 2005. What is Feline Infectious Peritonitis (FIP). Catvirus.com. Available Source: http://www.dr-addie.com/WhatIsFIP.htm, January 4, 2006.

_____ and C.E. Green. 1998. **Infectious Disease of the Dog and Cat**, 3 nd Ed., W.B. Saunders Co., Philadelphia, Pennsylvania.

_____, S. Paltrinieri and N.C. Pedersen. 2004. Recommendations from Workshops of the Second International Feline Coronavirus/Feline Infectious Peritonitis Symposium. **J. Feline Med. Sur.** 6: 125-130.

An, S., A. Maeda and S. Makino. 1998. Coronavirus Transcription Early in Infection. **J. Virol.** 72: 8517-8524.

Andrew, S.E. 2000. Feline Infectious Peritonitis. **Vet. Clin. North. Am. Small. Anim. Pract.** 30: 987-400.

Bell, E.T., J.A. Toribio, J.D. White, R. Malik and J.M. Norris. 2006. Seroprevalence Study of Feline Coronavirus in Owned and Feral Cats in Sydney, Australia. **Aust. Vet. J.** 84(3): 74-81.

Benbacer, L., E. Kut, L. Besnardeau, H. Laude and B. Dalmas. 1997. Interspecies Aminopeptidase-N Chimeras Reveal Species-Specific Receptor Recognition by Canine Coronavirus, Feline Infectious Peritonitis Virus, and Transmissible Gastroenteritis Virus. **J. Virol.** 71: 734-737.

Benetka, V., A. Kubber-Heiss, J. Kolodziejek, N. Nowotny, M. Hofmann-Parisot and K. Mostl. 2004. Prevalence of Feline Coronavirus Type I and II in Cats with

Histopathologically Verified Feline Infectious Peritonitis. **Vet. Microbiol.** 99: 31-42.

Biogal Galed Laboratories. 2004. Feline Corona Virus Antibody Test Kit. ImmunoComb. Available Source: http://www.biogal.co.il/products/pdf-mi/feline/FCoV%20.pdf, June 6, 2006.

Cave, T.A., M.C. Golder, J. Simpson and A.D. Addie. 2004. Risk Factors for Feline Coronavirus Seropositivity in Cats Relinquished to a UK Rescue Charity. **J. Feline Med. Sur.** 6: 53-58.

Chang, R.Y., M.A. Hofmann, P.B. Sethna and D.A. Brian. 1994. A *cis*-Acting Function for the Coronavirus Leader in Defective Interfering RNA Replication. **J. Virol.** 68: 8223-8231.

Corapi, W.V., R.J. Darteil, J.C. Audonnet and G.E. Chappais. 1995. Localization of Antigenic Sites of the S Glycoprotein of Feline Infectious Peritonitis Virus Involved in Neutralization and Antibody-Dependent Enhancement. **J. Virol.** 69: 2858-2862.

Dean, G.A., T. Olivry, C. Stanton and N.C. Pedersen. 2003. In vivo Cytokine Response to Experimental Feline Infectious Peritonitis Virus Infection. **Vet. Microbiol.** 97: 1-12.

Delmas, B. and H. Laude. 1990. Assembly of Coronavirus Spike Protein into Trimers and Its Role in Epitope Expression. **J. Virol.** 64: 5367-5375.

Ficus, S.A., B.L. Rivoire and Y.A. Teramoto. 1987. Epitope-Sepecific Antibody Responses to Virulent and Avirulent Feline Infectious Peritonitis Virus Isolates. **J. Clin. Microbiol.** 25: 1529-1534.

_____ and Y.A. Teramoto. 1987. Antigenic Comparison of Feline Coronavirus Isolates: Evidence for Markedly Different Peplomer Glycoproteins. **J. Virol.** 61: 2607-2617.

Flint, S.J., V.R. Racaniello, L.W. Enquist, A.M. Skalka and R.M. Krug. 2000. **Principles of Virology Molecular Biology, Pathogenesis, and Control.** American Socicty for Microbiology, Washington, DC.

Foley, J.E. and C. Leutenegger. 2001. A Review of Coronavirus Infection in the Central Nerovous System of Cats and Mice. **J. Vet. Intern. Med.** 15: 438-444.

Gallarher, T.M., C. Escarmis and M.J. Buchmeier. 1991. Alteration of the pH Dependence of Coronavirus-Induced Cell Fusion: Effect of Mutations in the Spike Glycoprotein. **J. Virol.** 65: 1916-1928.

_____, S.E. Parker and M.J. Buchmeier. 1990. Neutralization-Resistant Variants of Neurotropic Coronavirus are Generated by Deletions within the Amino-Terminal Half of the Spike Glycoprotein. **J. Virol.** 64: 731-741.

Gamble, D.A., A. Lobbiani, M. Gramegna, L.E. Moore and G. Colucci. 1997. Development of a Nested PCR Asssay for Detection of Feline Infectious Peritonitis Virus in Clinical Specimens. **J. Clin. Microbiol.** 35: 673-675.

Godeke, G.J., C.A. Hann, J.W. Rossen, H. Vennema and P.J. Rottier. 2000. Assembly of Spikes into Coronavirus Particles is Mediated by the Carboxy-Terminal Domain of the Spike Protein. **J.Virol.** 74: 1566-1571.

Godet, M., J. Grosclaude, B. Delmas and H. Laude. 1994. Major Receptor-Binding and Neutralization Determinants are Located within the Same Domain of the Transmissible Gastroenteritis Virus (Coronavirus) Spike Protein. **J. Virol.** 68: 8008-8016.

Gombold, J.L., S.T. Hingley and S.R. Weiss. 1993. Fusion-Defective Mutants of Mouse Hepatitis Virus A59 Contain a Mutation in the Spike Protein Cleavege Signal. **J. Virol.** 67: 4504-4512.

Greene, C.E. 1998. **Infectious Disease of the Dog and Cat.**. 2nd ed. W.B. Saunders, Philadelphia, PA.

Gunn-Moore, D.A., S.M. Caney, T.J. Gruffydd-Jones, C.R. Helps and D.A. Harbour. 1998. Antibody and Cytokine Responses in Kittens during the Development of Feline Infectious Peritonitis. **Vet. Immunol. Immunopathol.** 65: 221-242.

Gut, M., C.M. Leutenegger, J.B. Huder, N.C. Pedersen and H. Lutz. 1999. One-Tube Fluorogenic Reverse Transcription-Polymerase Chain Reaction for Quantitation of Feline Coronavirus. **J. Virol. Met.** 77: 37-46.

Haagmans, B.L., H.F. Egberink and M.C. Horzinek. 1996. Apoptosis and T-Cell Depletion Durine Feline Infectious Peritonitis. **J. Virol.** 70: 8977-8983.

Haan, C.A., L. Kuo, P.S. Masters, H. Vennema and P.J. Rottier. 1998. Coronavirus Particle Assembly: Primary Structure Requirements of the Membrane Protein. **J.Virol.** 72: 6838-6850.

Hegyi, A. and A.F. Kolb. 1998. Characterization of Determinants Involved in the Feline Infectious Peritonitis Virus Receptor Function of Feline Aminopeptidase N. **J. Gen. Virol.** 79: 1387-1391.

Herrewegh, A.P., I. Smeenk, M.C. Horzinek, P.J. Rottier and R.J. Groot. 1998. Feline Coronavirus Type II Strain 79-1683 and 79-1146 Originate from a Double Recombination between Feline Coronavirus Type I and Canine Coronavirus. **J.Virol.** 72: 4508-4514.

_____, R.J. Groot, A. Cerpica, H.F. Egberink, M.C. Horzinek and P.J. Rottier. 1995. Detection of Feline Coronavirus RNA in Feces, Tissues, and Body Fluids of Naturally Infected Cats by Reverse Transcriptase PCR. **J. Clin. Microbiol.** 33: 684-689.

Hingley, S.T., I. Leparc-Goffart and S.P. Weiss. 1998. The Spike Protein of Murine Coronavirus Mouse Hepatitis Virus Strain A59 is Not Cleaved in Primary Glial Cells and Primary Hepatocytes. **J.Virol.** 72: 1606-1609.

Hofmann, M.A., P.B. Sethna and D.A. Brian. 1990. Bovine Coronavirus mRNA Replication Continues throughout Persistent Infection in Cell Culture. **J. Virol.** 64: 4108-4114.

Hohdatsu, T., M. Yamada, R. Tominaga, K. Makino, K. Kida and H. Koyama. 1998 a. Antibody-Dependent Enhancement of Feline Infectious Peritonitis Virus Infection in Feline Alveolar Macrophages and Human Monocyte Cell Line U937 by Serum

of Cats Experimentally or Naturally Infected with Feline Coronavirus. **J. Vet. Med. Sci.** 60: 49-55.

_____, S. Okada, Y. Ishizuka, H. Yamada and H. Koyama. 1992. The Prevalence of Type I and II Feline Coronavirus infections in cats. **J. Vet. Med. Sci.** 3: 557-562.

_____, Y. Izumiya, Y. Yokoyama, K. Kida and H. Koyama. 1998 b. Differences in Virus Receptor for Type I and Type II Feline Infectious Peritonitis Virus. **Arch. Virol.** 143: 839-850.

Holst, B.S., L. Englund, S. Palacios, L. Renstrom and L.T. Berndtsson. 2006. Prevalence of Antibodies Against Feline Coronavirus and *Chlamydophila felis* in Swedish Cats. **J. Feline Med. Sur.** 8: 207-211.

Horzinek, M.C. and A. Herrewegh. 1995. Perspectives on Feline Coronavirus Evolution. **Feline Pract.** 23: 34-39.

_____ and A.D. Osterhaus. 1979. The Virology and Pathogenesis of Feline Infectious Peritonitis. **Arch. Virol.** 59: 1-15.

_____ and H. Lutz. 2001. An Update on Feline Infectious Peritonitis. Virology. Available Source: http://www.vetscite.org/issue1/reviews/txt_index_0800.htm, January 4, 2006.

Hoshino, Y. and F.W. Scott. 1980. Immunofluorescent and Electronmicroscopic Studies of Feline Small Intestine Organ Cultures Infected with Feline Infectious Peritonitis Virus. **Am. J. Vet. Res.** 41: 672-681.

Hoskins, J.D. 1993. Coronavirus Infection in Cats. **Vet. Clin. North. Am. Small. Anim. Pract.** 23: 1-16.

Jeong, Y.S. and S. Makino. 1994. Evidence for Coronavirus Discontinuous Transcription. **J. Virol.** 68: 2615-2623.

Joo, M. and S. Makino. 1992. Mutagenic Analysis of the Coronavirus Intergenic Consesus Sequence. **J. Virol.** 66: 6330-6337.

Kennedy, M., N. Boedeker, P. Gibbs and S. Kania. 2001. Deletions in the 7a ORF of Feline Coronavirus Associated with an Epidemic of Feline Infectious Peritonitis. **Vet. Microbiol.** 81: 227-234.

_____, S. Citino, A.H. McNabb, A.S. Moffatt, K. Gertz and S. Kania. 2002. Detection of Feline Coronavirus in Captive Felidae in the USA. **J. Vet. Diagn. Invest.** 14(6): 520-522.

Klumperman, J., J.K. Locker, A. Meijer, M.C. Horzinek, H.J. Geuze and P.J. Rottier. 1994. Coronavirus M Proteins Accumulate in the Golgi Complex beyond the Site of Virion Budding. **J. Virol.** 68: 6523-6534.

Kuo, L., G.J. Godeke, M.J.B. Raamsman, P.S. Masters and P.J. Rottier. 2000. Retargeting of Coronavirus by Substitution of the Spike Glycoprotein Ectodomain: Crossing the Host Cell Species Barrier. **J.Virol.** 74: 1393-1406.

Lai, M.M.C. and K.V. Holmes. 2001. *Coronaviridae*: The Viruses and Their Replication, pp. 1163-1185. *In* D.M. Knipe, P.M. Howley, D.E. Griffin, R.A. Lamb and M.A. Martin, eds. **Fields Virology**. 4th edition. Lippincott Williams and Wilkins, Philadelphia.

Liao, C. and M.M.C. Lai. 1994. Requirement of the 5'-End Genomic Sequence as an Upstream *cis*-Acting Element for Coronavirus Subgenomic mRNA Transcription. **J. Virol.** 68: 4727-4737.

Lin, Y.J., C.L. Liao and M.M.C. Lai. 1994. Identification of the *cis*-Acting Signal for Minus-Strand RNA Synthesis of a Murine Coronavirus: Implications for the Role of Minus-Strand RNA in RNA Replication and Transcription. **J. Virol.** 68: 8131-8140.

Liu, D.X. and S.C. Inglis. 1992. Internal Entry of Robosomes on a Tricistronic mRNA Encoded by Infectious Bronchitis Virus. **J. Virol.** 66: 6143-6154.

Most, R.G., R.J. de Groot and W.J.M. Spaan. 1994. Subgenomic RNA Synthesis Directed by a Synthetic Defective Interfering RNA of Mouse Hepatitis Virus: A Study of Coronavirus Transcription Initiation. **J. Virol.** 68: 3656-3666.

Martinez, M.L. and R.C. Weiss. 1993. Detection of Feline Infectious Peritonitis Virus Infection in Cell Cultures and Peripheral Blood Mononuclear Leukocytes of Experimentally Infected Cats Using a Bionylated cDNA probe. **Vet Microbiol.** 34: 259-271.

Masters, P.S., C.A. Koetzner, C.A. Kerr and Y. Heo. 1994. Optimization of Targeted RNA Recombination and Mapping of a Novel Nucleocapsid Gene Mutation in the Coronavirus Mouse Hepatiitis Virus. **J. Virol.** 68: 328-337.

Motokawa, K., T. Hohdatsu, H. Hashimoto and H. Koyama. 1996. Comparison of the

Amino Acid Sequence and Phylogenetic Analysis of the Peplomer, Integral Membrane and Nucleocapsid Protein of Feline, Canine and Porcine Coronaviruses. **Microbiol. Immunol.** 6: 425-433.

Paltrinieri, S., M.P. Cammarata, G. Cammarata and S. Comazzi. 1998. Some Aspects of Humoral and Cellular Immunity in Naturally Occurring Feline Infectious Peritonitis. **Vet. Immunol. Immunopathol.** 65: 205-220.

_____, S. Comazzi, V. Spagnolo and A. Giordano. 2002. Laboratory Changes Consistent with Feline Infectious Peritonitis in Cats from Multicat Environments. **J. Vet. Med.** 49: 503-510.

Poland, A.M., H. Vennema, J.E. Foley and N.C. Pedersen. 1996. Two Related Strains of Feline Infectious Peritonitis Virus Isolated from Immunocompromised Cats Infected with a Feline Enteric Coronavirus. **J. Clin. Microbiol.** 34: 3180-3184.

Pedersen, N.C. 1976. Serologic Studies of Naturally Occurring Feline Infectious Peritonitis. **Am. J. Vet. Res.** 37: 1449-1453.

_____. 1988. **Feline Infectious Disease**. American Veterinary Publications, Goleta, CA.

_____. 1995. An Overview of Feline Enteric Coronavirus and Infectious Peritonitis Virus Infection. **Feline Pract.** 23: 7-12.

_____. 2001. Coronavirus Diseases. Viral Diseases. Available Source: http://www. vetscite.org /issue1/reviews/txt_index_0800.htm, January 4, 2006.

Pedersen, N.C., J.F. Boyle, K. Floyd, A. Fudge and J. Barker. 1981. An Enteric Coronavirus Infectious of Cats, and Its Relationship to Feline Infectious Peritonitis. **Am. J. Vet. Res.** 42: 368-377.

_____, J.F. Evermann, A.J. Mckeirnan and R.L. Ott. 1984. Pathogenicity Studies of Feline Coronavirus Isolates 79-1146 and 79-1683. **Am. J. Vet. Res.** 45: 2580-2585.

Pesteanu-Somogyi, L.D., C. Radzai and B.M. Pressler. 2006. Prevalence of Feline Infectious Peritonitis in Specific Cat Breeds. **J. Feline Med. Sur.** 8: 1-5.

Qiagen. 2001. RNeasy Mini Handbook. Qiagen. Available Source: http://molecool. wustl.edu/krolllab/PDFs/Total%20RNA%20prep-Qiagen.pdf, January 20, 2006.

Rottier, P.J. 1999. The Molecular Dynamics of Feline Coronaviruses. **Vet. Microbiol.** 69: 117-125.

Routledge, E., R. Stauber, M. Pfleiderer and S.G. Siddell. 1991. Analysis of Murine Coronavirus Surface Glycoprotein Function by Using Monoclonal Antibodies. **J. Virol.** 65: 254-262.

Ruey-Yi, C., A.H. Martin, B.S. Phiroze and A.B. David. 1994. A Cis-Acting Function for the Coronavirus Leader in Defective Interfering RNA Replication. **J. Virol.** 68: 8223-8231.

Savary, K.C., R.K. Sellon and J.M. Law. 2001. Chylous Abdominal Effusion in Cat with Feline Infectious Peritonitis. **J. Am. Anim. Hosp. Assoc.** 37: 35-40.

Sethna, P.B., M.A. Hofmann and D.A. Brian. 1991. Minus-Strand Copies of Replicating Coronavirus mRNAs Contain Antileaders. **J. Virol.** 65: 320-325.

_____, S.L. Hung and D.A. Brian. 1989. Coronavirus Subgenomic Minus-Strand RNAs and the Potential for mRNA Replicons. **Proc. Natl. Acad. Sci. USA.** 86: 5626-5630.

Simons, F.A., H. Vennema, J.E. Rofina, J.M. Pol, M.C. Horzinek, P.J. Rottier and H.F. Egberink. 2005. A mRNA PCR for the Diagnosis of Feline Infectious Peritonitis. **J. Virol. Met.** 124: 111-116.

Stoddart, C.A. and F.W. Scott. 1989. Intrinsic Resistance of Feline Peritoneal Macrophages to Coronavirus Infection Correlated with *in vivo* Virulence. **J. Virol.** 1: 436-440.

Stohlman, S.A., R.S. Baric, G.N. Nelson, L.H. Soe, L.M. Welter and R.J. Deans. 1988. Specific Interaction between Coronavirus Leader RNA and Nucleocapsid Protein. **J. Virol.** 62: 4288-4295.

Sturman, L.S., C.S. Ricard and K.V. Holmes. 1990. Conformational Change of the Coronavirus Peplomer Glycoprotein at pH 8.0 and 37^{o}C Correlates with Virus Aggregation and Virus-Induced Cell Fusion. **J. Virol.** 64: 3042-3050.

_____, K.V. Holmes and J. Behnke. 1980. Isolation of Coronavirus Envelope Glycoproteins and Interaction with the Viral Nucleocapsid. **J. Virol.** 33: 449-462.

Tooze, J., S. Tooze and G. Warren. 1984. Replication of Coronavirus MHV-A59 in Sac Cells: Determination of the First Site of Budding of Progeny Virions. ***Eur. J. Cell. Biol.*** 33: 281-293.

Tresnan, D.B., R. Levis and K.V. Holemes. 1996. Feline Aminopeptidase N Serves as a Receptor for Feline, Canine, Porcine and Human Coronavirus in Serogroup I. **J. Virol.** 70: 8669-8674.

Tyrrell, D.A.J. and S.H. Myint. 2006. Coronaviruses. Medical Microbiology. Available Source: http://gsbs.utmb.edu/microbook/ch060.htm, January 4, 2006.

Vennema, H., A. Poland and K.F. Hawkins. 1995. A Comparison of the Genomes of FECVs and FIPVs and What They Tell Us about the Relationships between Feline Coronaviruses and Their Evolution. **Feline Pract.** 23: 40-44.

_____, A. Poland, J.E. Foley and N.C. Pedersen. 1998. Feline Infectious Peritonitis Viruses Arise by Mutation from Endemic Feline Enteric Coronavirus. **Virology.** 243: 150-157.

_____, G.J. Godeke, J.W. Rossen, W.F. Voorhout, M.C. Horzinek, D.J. Opstelten and P.J. Rottier. 1996. Nucleocapsid-Independent Assembly of Coronavirus-Like Particles by Co-Expression of Viral Envelope Protein Genes. ***EMBO. J.*** 15: 2020-2028.

_____, L. Heijnen, A. Zijderveld, M.C. Horzinek and W.J. Spaan. 1990. Intracellular Transport of Recombinant Coronavirus Spike Proteins: Implications for Virus Assembly. **J. Virol.** 64: 339-346.

Woo, K., M. Joo, K. Narayanan, K.H. Kim and S. Makino. 1997. Murine Coronavirus Packaging Signal Confers Packaging to Nonviral RNA. **J. Virol.** 71: 824-827.

Yi-Jyun, L., L. Ching-Len and M.C. Michael. 1994. Identification of the Cis-Acting Signal for Minus-Strand RNA Synthesis of a Murine Coronavirus: Implications for the Role of Minus-Strand RNA in RNA Replication and Transcription. **J. Virol.** 68: 8131-8140.

Yokomori, K., L.R. Banner and M.M.C. Lai. 1992. Coronavirus mRNA Transcription: UV Light Transcription Mapping Studies Suggest an Early Requirement for a Genomic-Length Template. **J. Virol.** 66: 4671-4678.

Zhang, X., C. Liao and M.M.C. Lai. 1994. Coronavirus Leader RNA Regulates and Initiates Subgenomic mRNA Transcription both in *trans* and in *cis*. **J. Virol.** 68: 4738-4746.

Zelus, B.D., J.H. Schickli, D.M. Blau, S.R. Weiss and K.V. Holmes. 2003. Conformational Changes in the Spike Glycoprotein of Murine Coronavirus are Induced at 37^{o}C either by Soluble Murine CEACAM1 Receptors or by pH8. **J. Virol.** 77: 830-840.

APPENDIX

Appendix

Preparation of Reagent and Buffers

1. 0.5 M EDTA (pH 8.0)

To 800 ml of distilled water, 186.1 g of disodium ethylenediaminetetraacetate. $2H_2O$ was added and stirred vigorously on a magnetic stirrer. The pH was adjusted to 8.0 with NaOH (20g of NaOH pellets). The volume was adjusted to 1 litter. The solution was dispensed into aliquots and sterilized by autoclaving for 15 minutes at 15 lb/in^2.

2. Ethidium bromide solution (10 mg/ml)

The ethidium bromide solution was prepared by dissolving 1 g of ethidium bromide in 100 ml of distilled water. The solution was stored in light-tight container at room temperature.

3. Tris-acetate (TAE) buffer

1xTAE buffer was used as an electrophoresis buffer throughout the study. The working solution of 1xTAE buffer was prepared from stock solution of 50xTAE buffer, as followed.

50xTAE buffer :	Tris-base	242 g
	Glacial acetic acid	57.1 ml
	0.5 M EDTA (pH 8.0)	100 ml
	Distilled water, adjust to	1 L